Peabody Museum
of Natural History
Yale University
New Haven, Ct. 06520

Postilla Number 173
12 April 1978

Osteology of the American Plaice, Hippoglossoides platessoides*

David W. Frame
Thomas J. Andrews
Charles F. Cole

Memorial

On 8 September 1973 Dr. David W. Frame, this paper's senior author and our close friend and research-colleague died during a boating accident near Beaufort, North Carolina. This tragic event terminated a productive and rewarding relationship David had with us and one that the junior authors wish to memorialize. After graduating from Ohio University, David entered the University of Massachusetts in September 1965 and in May 1968 received his Master of Science with a thesis entitled "The epibiota attached to wooden panels in the Cape Cod Canal, Sandwich, Massachusetts." In the fall of 1968 David began his doctoral program with a three months' cruise on *Te Vega* off western South and Central America. Out of this cruise developed his interests in comparative anatomy and in the ecology of tropical flounders. This present paper, an outgrowth of our collective interest in the comparative anatomy of a North Atlantic flounder, was to have been the basis for a continuing osteological review of flounder genera on a world-wide basis. David completed the Ph.D. in Fisheries Biology in October 1971 at the University of Massachusetts, with a dissertation entitled "Biology of young winter flounder, *Pseudopleuronectes americanus* (Walbaum): feeding habits, metabolism and food utilization." Two papers from this dissertation appeared in the *Transactions of the American Fisheries Society* (1973). His last position was Fishery Biologist at the Atlantic Estuarine Fisheries Center, Beaufort, North Carolina.

During his professional life David exhibited a wide interest in the sea and in the biology of its fishes. We who shared in his education fully expected that his professional career would be both long and productive. Though this did not occur, his passage through our own teaching careers was one marked by high scholarship standards and a drive for professional perfection. We thus note with great sorrow the passing of our friend.

Abstract

The *Hippoglossoides platessoides* skeleton is described and figured; for these purposes 17 specimens were observed. Study material was prepared by fleshing and disarticulation or by clearing and staining. Skull lengths of the specimens examined ranged from 27 to 68 mm and total lengths from 181 to 851 mm.

Paired lacrymals constitute the only suborbital elements, although canal ossicles occur on both sides. A single nasal houses a portion of the supraorbital lateral-line canal of the right eye. Right elements of the oromandibular region are anterior and ventral to their left counterparts. Three left jaw bones, premaxillary, maxillary and dentary, are longer than the right elements. Tooth-bearing structures are represented by the premaxillaries, dentaries, pharyngobranchials (2–4) and ceratobranchials (5). The spine of the neural process of the first trunk vertebra extends well above the cranium whereas its arch in part lies sessile on

*Contribution No. 41 of the Massachusetts Cooperative Fishery Research Unit jointly sponsored by the U.S. Fish and Wildlife Service, the Massachusetts Division of Fisheries and Wildlife, the Massachusetts Division of Marine Fisheries, and the University of Massachusetts.

the second centrum. Additional pleural and epipleural ribs may be found on the right side. Lateral apophyses are confined to the right side but arise from trunk and caudal centra. The specialized caudal skeleton consists of 18 branched lepidotrichs, 1 parhypural, 2 hypural plates and 2 epurals.

Introduction

The genus *Hippoglossoides* Gottsche, 1835, contains a single species in the North Atlantic, *Hippoglossoides platessoides* (Fabricius) 1780, ranging from Cape Cod to Greenland and then to England. According to Gill (1864, p. 217) the lateral-line description was wholly misleading because Fabricius stated, "Linea lateralis humilior, recta medietatem oculorum spectat, ventriculum tamen arcu ambiens angulo aperaturae branchialis summo terminata . . ." whereas the line is nearly straight. With the latter notation, Gill (1864) placed this species in the genus *Hippoglossoides.* However, neither investigator described the osteological features that set this species apart from other pleuronectids.

One of the earliest accounts of the cranial osteology asymmetry of the family Pleuronectidae was presented by Traquair (1865). He described the cranial features of the three species *(Hippoglossus hippoglossus, Reinhardtius hippoglossoides,* and *Pleuronectes platessa),* but the most comprehensive examination of the family Pleuronectidae to date has been conducted by Chabanaud (1933, 1934, 1935, 1936, 1938). His papers dealing with the asymmetry of the neurocranium substantiate Regan's (1910) hypothesis that the Heterosomata (= Pleuronectiformes) are related to the Perciformes. Prior to this time, Cope (1871) and Jordan and Evermann (1898) regarded them as gadoid relatives.

The flatfish caudal skeleton has been described by Whitehouse (1910) and Barrington (1937), though their accounts do not postulate the phylogenetic trends leading from perciform stock. Works of Hollister (1937) and Gosline (1961) clearly demonstrate that evolution of the caudal skeleton in modern teleosts is toward reduction and simplification by fusion of elements. The structural relationships in this complex existing between pleuronectids and perciforms had been emphasized by Monod (1968) and Rosen and Patterson (1969).

In undertaking this study we intend to present the detailed osteological description that Cope neglected to provide in his designation of the generic taxon. Future reviews confined to pleuronectid systematics must take into account variations that have evolved in the endoskeleton. This description of the plaice, *H. platessoides,* contributes to a thorough revision of *Hippoglossoides* and related genera.

Methods and Materials

Terminology of bones follows that of several authors: the osteocranium, Harrington (1955); the appendicular skeleton and vertebral column, Norden (1961) and Ford (1937), respectively; the caudal skeleton, generally Gosline (1961), Monod (1968), and Rosen and Patterson (1969) with exceptions noted in the text. Specimens were either fresh-frozen or preserved in 10% formalin prior to reduction that involved one of three methods: (1) fleshing of the skeleton (Konnerth, 1965); (2) clearing in 4% KOH and staining with alizarin red; (3) clearing in trypsin and staining with alizarin red. The format of this communication follows that of Topp and Cole (1968). Seventeen specimens were examined (Table 1). Drawings were prepared using a Kail Reflecting Projector, Model K-5.* An alphabetic list of abbreviations appears below, for osteological elements and for other anatomical terms used in this work.

Standard terminology referrring to the position of each element is used throughout the text. Although the midsagittal or median plane divides the fish into equal halves, cephalic structures lying in this plane are not always symmetrically equivalent due to the torsional development of the flatfish skull.

Anatomical Abbreviations

ac actinost
an angular
apv antepenultimate vertebra
art retroarticular
b branchiostegal

*Use of this piece of equipment does not constitute an endorsement by the NMFS.

Table 1. Specimen Preparation and Dimensions

Specimen Number	Description of Preparation	Skull Length (mm)*	Standard Length (mm)
1	Syncranium; girdles and vertebrae completely disarticulated and cleaned.	64	778
2	Neurocranium, hyoid and branchial arches; anal and median fins disarticulated and cleaned.	68	782
3	Olfactory region of neurocranium dissected. Pectoral girdle and trunk vertebrae disarticulated.	39	239
4	Disarticulated pleural ribs and trunk vertebrae.	37	227
5	Disarticulated pleural ribs and trunk vertebrae.	38	231
6	Caudal skeleton and vertebral column cleaned and intact.	42	244
7	Caudal skeleton and vertebral column cleaned and intact.	38	217
8-14	Cleared in .04 percent N potassium hydroxide and stained; specimens disarticulated.		187 219 145 142 140 218 170
15	Cleared in trypsin, skeleton intact.	29	172
16	Cleared in trypsin, olfactory region caudal skeleton disarticulated.	33	206
17	Cleared in trypsin, mandibles disarticulated.	27	157

*Skull length (mm) represents the distance from the prevomer to the right epiotic.

bb1—bb3 basibranchial
bh basihyal
boc basioccipital
bpt basipterygium, pelvic girdle
cb1–cb5 ceratobranchial
ch ceratohyal
cl cleithrum
cor coracoid
d dentary
dpt distal pterygiophore
e ethmoid
eb1–eb4 epibranchial
eh epihyal
enp endosteal process
enpt endopterygoid
eoc exoccipital
epo epiotic
epp lateral apophysis
epr epipleural rib
eu1–eu2 epural, caudal fin
f frontal
fle first lateral extrascapula
fn interorbital fenestra
g gill raker
hb1–hb3 hypobranchial
hfa hyomandibular facet
hfo hyomandibular fossa
hs haemal spine
hu1–hu2 hypural plate
hyo hyomandibular
ih interhyal
ihs interhaemal spine
iop interopercular
ipt intermediate pterygiophore
l lacrymal
le lateral ethmoid
lep lepidotrich
lhh lower hypohyal
mc Meckel's cartilage
mpt metapterygoid
mx maxillary
n nasal
nf spinal nerve foramen
npoz neural postzygapophysis
nprz neural prezygapophysis
ns neural spine
op opercular
opo opisthotic

pa parietal
par parapophysis
pb1–pb4 pharyngobranchial
pc primordial cartilage
pcl postcleithrum
pf prefrontal
phu parhypural
pl autopalatine
pmx premaxillary
pop preopercular
ppt proximal pterygiophore
pr pleural rib
pro prootic
psp parasphenoid
pt posttemporal
pto autopterotic
ptr ectopterygoid
pts pterosphenoid
pv penultimate vertebra
qu quadrate
r rostral process
sa coronomeckelian
sc scapula
scl supracleithrum
soc supraoccipital
sop subopercular
spo autosphenotic
sym symplectic
tv terminal vertebra
uhh upper hypohyal
urh urohyal
v prevomer

Description of Skeleton

Neurocranium

Olfactory Region

This asymmetrical region consists of two paired bones: lateral ethmoids, prefrontals and three unpaired bones—ethmoid, prevomer, and nasal.

Ethmoid (Fig. 3A,*e*) This endochondral bone is recessed craniad and fused to the right lateral ethmoid ventrally and right prefrontal dorsolaterally. Prefrontals are tightly sutured dorsally and dorsolaterally. These sutures are indistinguishable in adults, and the ethmoid could easily be overlooked were it not for the anteromedial keel projecting rostrad, and for the visible sutures in smaller specimens. In *Hippoglossus hippoglossus* the former projection apparently represents a median-ridge lower in profile than the one found in *H. platessoides* (Yazdani, 1969). Although partially hidden by the prevomer, the cartilaginous connection to the keel comprises the anterior-most portions of the primordial cartilage (Fig. 2B) of the rostrum (Starks, 1926). Also hidden from the anterior view by the prevomer is the anterior portion of the interorbital fenestra outlined by the surrounding rostral cartilage.

Three foramina are situated below the ethmoid keel. One pierces each lateral ethmoid (the foramen of the left lateral ethmoid is hidden from view in Fig. 3A), to allow passage of the olfactory nerve, whereas the remaining ethmoid foramen is poorly developed in small specimens and is nearly closed in older animals by the primordial cartilage (Fig. 2B: *pc*) of the interorbital septum (Kyle, 1921).

Lateral ethmoids (Figs. 1; 2A,B,C; 3A: *le*) The asymmetry of the olfactory region is heightened by these two dissimilar endochrondral elements, one located ventrally (right) the other dorsolaterally (left). The right deltoid bone is fused to the frontal and prefrontal, lateral to the ethmoid, while the L-shaped left element is fused cranially to the prefrontal. Both lateral ethmoids contact the winged process of the prevomer. An extension of the left lateral ethmoid posteriorly borders the interorbital fenestra (Fig. 2c: *fn*) reaching the parasphenoid. The rostral cartilage (hidden from anterior view) is attached to the ethmoid and borders both lateral ethmoids.

The internal ventral margin of the left lateral ethmoid, rostral to the primordial cartilage of the interorbital septum, supports the origin of two branches of the superior oblique muscle to each eye.

Prefrontals (Figs. 1; 2A,B,C; 3A: *pf*) The curved dermal prefrontals protect the anterior portion of the orbits. In right lateral aspect, the right prefrontal appears fan shaped and is weakly sutured to the larger left prefrontal. An endorbital splint from the left lateral ethmoid

contacts the two prefrontals along their common suture (hidden from view by the anterior prefrontal, lateral view).

Prevomer (Figs. 1; 2A,B,C; 3A: *v*) The dermal edentulous prevomer consists of a fist-shaped head with lateral wing-like projections supported by the lateral ethmoids. A spline directed posteriorly from the head locks into the parasphenoid. The left lateral view shows portions of the prevomer spline and the parasphenoid contributing to the margin of the interorbital fenestra (Kyle, 1921). The rostral cartilage is denied contact with the prevomer head which is twisted to the left. Ventrolateral to the prevomer head are two groove-shaped excavations where the autopalatines are closely applied. The anterior portion of each autopalatine contacts, syndesmotically, the mesial process of the maxillary and not the prevomer.

Nasal (Figs. 1; 4:*n*) This canal-bearing cylindrical element is located in the cutis, anterior to the right prefrontal. The bone arcs anterolaterally and is perforated by the canal that houses a segment of the right supraorbital lateral line nerve (ventral eye). The right suborbital lateral line traverses 14 minute tubular elements.

Orbital Region

This region is comprised of four paired bones: frontals, sclerotics, pterosphenoids, and lacrymals. The orbitosphenoid and all dermal elements of the suborbital series (except the lacrymals) are absent in this species.

Frontals (Figs. 1; 2A,B,C; 3A: *f*) These cancellous dermal elements contribute to the posterior borders of the left orbit and are ankylosed by a descending process directed ventrad from the left frontal. The latter bone assumes broad sutural contact with several elements (pterosphenoid, parasphenoid, supraoccipital and autosphenotic) while anteriorly providing primary support for the prefrontal. A single blind canal is present middorsally. The extensively canalized right frontal is in contact posteriorly with the pterosphenoid and supraoccipital but narrows anteriorly into a strut that supports both the prefrontal and lateral ethmoid. A lateral ridge present on each element bifurcates above the autosphenotics. The posterodorsal branch contacts the epiotic and the posteroventral branch is colinear with the autopterotic.

Lacrymals (Figs. 1; 4: *1*) The right suborbital element possesses a broad ridge on its mesial face that contacts the right lateral ethmoid via ligament. Its thin convex wings are asymmetrical, the anterior portion lanceolate, the posterior portion rounded. The left subrectangular element is anteroventral to the left prefrontal and possesses an open lateral groove. It represents the first of seven to nine small tubular bones enclosing the left suborbital lateral line (dorsal eye). The position of the lacrymals agrees with that of other pleuronectid species (Gregory, 1933; Yazdani, 1969). Paired ligaments extend from the anterolateral surface of the maxillary processes to the lacrymals (maxilla—1st infraorbital ligament of Yazdani, 1969). Both elements are ligamentously bound to the lateral ethmoid, but the right lacrymal supports additionally a branch of the mandibulo-maxillary ligament.

Sclerotics (not figured) A pair of partially ossified translucent hemispheres are located within each of the two eyes. The two halves, anterior and posterior to the pupil, constitute a complete sphere in natural juxtaposition.

Pterosphenoids (Fig. 2B,C: *pts*) These paired endochondral bones, coplanar with the cruciform winged processes of the parasphenoid, contact the autosphenotics dorsally, the prootics posteriorly, and the frontals anteriorly. A large oval foramen lies on the pterosphenoid and prootic suture and is shared equally by both elements. This opening allows the passage of the jugular vein (Aditus jugulaire of Chabanaud, 1936) and the trigeminal nerve, mandibular division. Mesially, the pterosphenoids are in contact by a transverse strut which arises from the internal face of each bone to meet midsagittally.

Although the transverse strut is fully ossified, its location is similar to the epiphyseal bar described by Harrington (1955). A second anterior foramen opens below the transverse strut and permits the passage of the trigeminal nerve, ophthalmic division.

Three eye muscles originate on both the right and left portions of the interpterosphenoid strut: the external occular rectus, left laterally; superior ocular rectus, mesial to the latter; and the internal ocular rectus medially. According to Chabanaud (1936) these muscles are inserted on the dorsal eye; the same complex is repeated on the right side for the ventral eye.

Otic Region

There are ten paired elements: autosphenotics, autopterotics, epiotics, prootics, opisthotics, exoccipitals, parietals, posttemporals, first lateral extrascapulae and a single supraoccipital.

Autosphenotics (Figs. 1; 2A,B,C: *spo*) The paired autosphenotics lie posterior to the frontals and contact their respective parietals mesially. Broad sutural contact is maintained with the pterosphenoids anteroventrally and the prootics posteroventrally. In older specimens sutures with the posterior autopterotics are indistinct. The overlying horizontal ridge of the pterosphenoid is colinear with the frontal, and the ventrolateral margin of the ridge together with autosphenotic provides a base for the origin of the first branch of the adductor mandibulae. This muscle is better developed on the left side and extends well over the frontal thereby occupying the space vacated by the migratory eye (Yazdani, 1969). The hyomandibular fossa (Fig. 2C: *hfo*) is a hemispheric recess posteroventral to a lateral tabular process from the autosphenotic. Within the fossa resides the autosphenotic-prootic suture; laterally the boundary is obscured by the fossa rim.

Autopterotics (Figs. 1; 2A,B,C; 3B: *pto*) Each element is bordered dorsally by the epiotic, posteriorly by the exoccipital and lies ventral to the opisthotic. Each bone as it progresses mediad contributes to the lateral relief.

A foramen for the passage of the cephalic lateral-line system pierces the dorsomesial surface of the ridge at its flexure. The former houses the otic branch, whereas the vertical canal protects the preopercular branch of the lateral-line system. Between the autopterotic and epiotic ridges lies the deeply excavated posttemporal fossa within which the first lateral extrascapula is ligamentously bound anteriorly. A ridge traversing both autopterotic and autosphenotic anchors the levator operculi. Ventromedial to the ridge is the hyomandibular facet (Fig. 2C: *hfa*) that extends posteriorly.

Prootics (Figs. 2B,C: *pro*) These are the largest endochondral bones of the otic series and are bordered by the parasphenoid ventrally and the opisthotics posteriorly. The autopterotics and autosphenotics are tightly sutured to the prootics. The mesial surface of each element maintains a lunar septum that marks the anterior margin of the sacular bulla containing the sacular otolith (sagitta). The septum is inclined posteriorly at an acute angle to the prootic and autosphenotic. Within the margin of the angle underlying the hyomandibular fossa (Fig. 2C: *hfo*) is a single ampullar recess.

A foramen located on the posteroventral border of each bone allows the passage of the internal carotid (Chabanaud, 1936). This opening is considerably larger on the right side. Dorsolaterally, a large elliptical foramen lies on the prootic-pterosphenoid suture and permits passage of the jugular vein and mandibular division of the trigeminal nerve. The facial nerve exits via an opening posterior to the jugular foramen.

The otoliths (sagittae) are large and compressed (Fig. 4). The two differ in shape — one possessing a tab on its margin, the other having an entire margin. Each is centrally grooved on one side but smooth on the convex face. Their appearance conforms to the otoliths figured by Norman (1934) for this species.

Opisthotics (Figs. 2B,C; 3B: *opo*) These are the last elements ossified in the otic region and in young specimens are the last cranial elements to form. They contribute to the posterodorsal cap of the auditory capsule. At the posterior border of the opisthotic is a foramen shared by the autopterotic and exoccipital, allowing passage of the glossopharyngeal nerve. Each convex element is bordered anteriorly by the prootic and dorsolaterally by the autopterotic. The exoccipitals posteriorly and the basioccipital posteroventrally also contact the margins of the opisthotics.

Epiotics (Figs. 1; 2A,C; 3B: *epo*) These endochondral elements meet mesially above the dorsoanterior margin of the exoccipitals. They are sutured to the autopterotics ventrolaterally and the supraoccipital dorsomesially. Bony apolamellae are supported by broad planar flanges that angle posteroventrally. These tabular processes support the posttemporal.

Exoccipitals (Figs. 2A,B,C; 3B: *eoc*) In posterior view the two cornual processes border the foramen magnum with their ventral broad portions terminating in compressed-elliptical facets. The inclined surfaces on their facets diverge at an angle of 100°. The foramen magnum is closed middorsally by the two epiotics, and midventrally by the basioccipital. A line extending from the low supraoccipital crest through the midcondylar surface of the basioccipital is dextrally convex (Kyle, 1921). This asymmetry, less pronounced than the anterior portion of the neurocranium, is enhanced by the larger right exoccipital together with the more anterior autopterotic that is laterally produced. In addition, the exoccipital-epiotic suture (posterior view) is nearly level on the right side but is curved on the left.

From the posterior cornual borders of the exoccipital two planar surfaces extend dorsolaterally and anterolaterally. The latter surface contributes to the posttemporal fossa. Above the condyles is an anteromesial foramen for the lateral passage of the vagus nerve.

Supraoccipital (Figs. 1; 2A; 3B: *soc*) A median low keel marks the position of this single carinate element. The bond is sutured to the frontals anterolaterally and its keel is confluent with a ridge on the left frontal. Parietals contact the lateral margins while the epiotics are sutured along the posterior and posterolateral borders. The supraoccipital caps the neurocranium.

Parietals (Fig. 1; 2A: *pa*) These thin elliptical dermal bones are sutured anteriorly to the frontals, medially to the supraoccipital and posterolaterally to the epiotics. The margin of each parietal reinforces the lateral ridge that extends posteriorly from the right frontal. The parietals can be easily overlooked in smaller specimens.

Posttemporals (Figs. 1; 12A, B: *pt*) These paired bones link the pectoral girdle with the cranium and are ligamentously bound to the posterolateral surfaces of the tabular processes (apolamellae) of the epiotics. The anterior portion of each bone is bifid, the dorsal extension articulating with the epiotic and the lower canalized branch is free. The latter canal houses the posttemporal branch of the lateral–line system and is contiguous with the horizontal canal of the first lateral extrascapula. According to Futch (personal communication), the second lateral extrascapula has become inseparably fused to the posttemporal, thus stabilizing its horizontal canal. The posterior lance-shaped portion of each bone articulates with the supracleithrum ventrolateral margin and is inserted on the posterodorsal margin of the operculum.

First lateral extrascapulae (Figs. 1; 4: *fle*) These canalized dermal elements are ligamentously attached to epiotics and autopterotics within the posttemporal fossa. The longer horizontal canal protects the postorbital and posttemporal branches of the cephalic lateral-line system, whereas a shorter vertical canal houses the supratemporal branch. Harrington (1955) and Futch (personal communication) have resolved the confusion concerning the position of the extrascapulae.

Basicranial Region

This portion of the osteocranium is occupied by two unpaired bones, the dermal parasphenoid and the endochondral basioccipital. This region contributes to the roof of the mouth and the floor of the braincase.

Basioccipital (Figs. 1; 2B,C; 3B: *boc*) The posterior portion of this element contains an oval, concave facet, which together with the exoccipital facets, provides broad support for the atlas. This bone contacts the opisthotics anterolaterally and the parasphenoid anteroventrally. It constitutes the primary supporting element in the braincase floor. Two cornual projections extend anterolaterally, their broad base contributing to the facet and their horns forming the posteroventral wall of the auditory capsule.

Parasphenoid (Figs. 1; 2B,C: *psp*) This bone, the largest skull bone, extends from the orbit, traverses the otic region midventrally and terminates on the basioccipital. It is the longest skull bone. The biramous anterior portion twists from ventral to lateral aspect and thus adds to the asymmetry of the anterior neurocranium (Kyle, 1921). It is sutured to the left frontal (not the right), the pterosphenoids, prootics and basioccipital. The prevomer spline locks neatly within the ventral branch and the left lateral ethmoid splint is appressed to the inner face of the dorsal parasphenoid branch. The primordial cartilage of the interorbital septum is attached to the bony web separating the two rami below the left lateral ethmoid.

The adductores arcus palatini originate along the bone's edge, posterior to the vomer and insert on the dorsal border of the endopterygoid and metapterygoid. Two prominent veins, from the rostral and mandibular regions meet the extramural jugular at the vomer-lateral ethmoid suture. The latter passes posteriorly along the lateral margin of the parasphenoid, above the muscle origin, to pass through the jugular foramen. In ventral view this bond is typically cruciform in appearance with its lateral processes meeting the prootic.

Branchiocranium

Oromandibular Region

Bones of this region contribute to the oral roof, protect the inner surface of the lower right orbit, and comprise the upper jaw and mandible. There are 12 paired bones (13 including the preopercular, commonly considered a bone of the hyoid region). There are 5 endochondral elements: autopalatines, quadrates, symplectics, metapterygoids and the retroarticulars of the mandible. The 8 dermal elements are, therefore, ectopterygoids, endopterygoids, premaxillaries, maxillaries, dentaries, angulars, preoperculars, and coronomeckelians. The asymmetry of this region has been described for other pleuronectids: Traquair (1865), Kyle (1921), Norman (1934), and Yazdani (1969). In *H. platessoides* the right oromandibular elements lie slightly anterior and ventral to their counterparts.

Autopalatines (Figs. 1; 5A,B: *pl*) These paired toothless bones represent the anteriormost endochondral derivatives of the oromandibular region. Each is sutured to the endopterygoid and ectopterygoid posteroventrally. The hammer-shaped, left autopalatine lies lateral to the prevomer and its planar head curves laterally to flank the maxillary process. The strutlike right autopalatine also curves anterolaterally to articulate with the underlying maxillary. The maxillary maintains a ligamentous connection with the premaxillaries.

Endopterygoids (Figs. 1; 5A,B: *enpt*) Each is a thin translucent bone, subrhomboidal in shape, lying above the ectopterygoid; its planar surface projects mesiad contacting the opposite endopterygoid midsagittally. Their buccal faces contribute to the support of palatal tissue. A narrow bony bridge provides primary support with the autopalatine anteriorly. Connective tissue (secondarily ossified in older specimens) exists peripherally with the metapterygoids and quadrates. The left element is considerably longer than the con-

tralateral, but the latter shields the ventromesial surface of the left orbit.

Ectopterygoid (Figs. 1; 5A,B: *ptr*) These boomerang-shaped splints support their respective autopalatines anteriorly and quadrates lateroventrally. Although similar in width, the right bone is stouter and has a less obtuse central angle. The dorsal arm is bordered by an ensiform projection extending anteriomesially from the quadrate. A broad sheet of tissue passes from the ventral margin to the maxillary on the left side, and between the right ectopterygoid to both lacrymal and maxillary of the right side.

Metapterygoids (Figs. 1; 5A,B: *mpt*) These thin, flat, translucent plates are sutured to their respective quadrates and are in planar contact with their symplectics and hyomandibulars via membranous ligaments. They are beveled medially and contain radiating ossified ridges. The right element is smaller than the left. No muscles are attached to their lateral faces, but the adductores arcus palatini are inserted dorsomesially.

Quadrates (Figs. 1; 5A,B: *qu*) These two bones are similar, but the right is slightly anterior and ventral to the left. Each triangulate quadrate possesses on its lower apex an obtuse condyle for reception of the angular. A strand of ligament posteroventral to the condyle, extends to the dorsolateral surface of the angular (mandibulo-quadrate ligament of Yazdani, 1969). The oblique posterior margin of each element is firmly attached to the preopercular and the symplectic passes into a dorsomedial recess in the triangle base. Posterodorsally, the metapterygoids are coplanar with the symplectics and quadrates. The anterior oblique border of the left quadrate is also colinear with the ectopterygoid.

Symplectics (Figs. 1; 5A,B: *sym*) Each cuneiform symplectic articulates posteriorly with the hyomandibular in a recess on the anteriomesial surface of the preopercular and extends anterioventrally to the quadrate. Approximately one-half of the left symplectic passes within the preopercular recess, whereas the right one does so for only about one-quarter of its length. This is clearly demonstrated in younger specimens cleared with 0.04 N potassium hydroxide, but in older fleshed specimens the thin symplectic tends to curl or flex laterally from its natural position.

Preopercular (Figs. 1; 5A,B: *pop*) These falciform dermal bones support the anterioventral quadrate-angular joints. Their margins are entire and exposed, covered only by a thin integumentary layer. The vertical portion of each element is supported throughout three-quarters of its length by the hyomandibular. The ventromesial margin of the remaining quarter and lower horizontal portion is occupied by the symplectic and quadrate. A branch of the adductor mandibularis originates along the vertical border overlying the hyomandibular and passes over the distal lateral surfaces of the metapterygoid, quadrate and ectopterygoid to insert on the dorsomesial margin of the angular anterior to the quadrate-angular fossa.

The lateral-line canal, internally, extends the length of the preopercular and is exposed by five fenestra. Dorsally, the sensory system traverses the autopterotic to pass into the preopercular canal. This latter canal exits through a foramen in the margin of the preopercular posterior to the quadrate condyle.

Dentaries (Figs. 1; 6A,B,C: *d*) These anterior bones of the mandible join at the anteromesial symphysis. Canine teeth line the dorsomesial edge of each element. In lateral aspect each ramus appears triangular with a unciform process extending ventrad from the anterior apex and with a lateral ridge extending to the acute anterior angle. The angular spline projects anteriorly within each dentary; the dentary covers about one-quarter of the angular spline which projects anteriorly into each dentary. The left dentary is one-third longer than the right; the latter element is slightly anterior and ventral to the former.

The mandibular lateral-line canal passes

within the dentary ventrally paralleling the lateral ridge. Four elliptical fenestrae open ventrolaterally and are therefore partly overshadowed by the ridge. This planar ventrolateral surface of the dentary forms the ventral surface of the jaw.

Angulars (Figs. 1; 6A,B,C: *an*) These endochondral elements support the dentaries anteriorly with interlocking trianguloid projections. Both right and left elements are similar in form and position, but the left angular spline is slightly longer. Each bone articulates with a quadrate condyle by means of a massive transverse fossa. On the internal face, each retains a strand of Meckel's cartilage (Fig. 6C: *mc*) extending from the endosteal process (Fig. 6C: *enp*) anteriomesially into the dentary with the underlying osseous projection. A small wedge of bone, the coronomeckelian, is located beneath the strand of Meckel's cartilage in a troughlike depression anterior to the endosteal process. The retroarticular is sutured to each bone posteroventrally. Dorsal to the latter element the mandibular lateralline nerve passes from the preopercular to traverse the external surface of the angular. The adductor mandibularis inserts on the dorsal margin of each element posterior to the coronoid process of the dentary and on the maxillary-retroarticular ligament.

Retroarticulars (Figs. 1; 6A,B,C: *art*) These paired bones cap the posteroventral margin of the mandible. Protruding from the inner surface of each element is a hollow conical process with vertex directed posteroventrally and orifice positioned beneath the hyomandibular fossa. The paired angulars do not differ in form. Mandibulo-interopercular and mandibulo-preopercular ligaments are attached to the posteroventral edge of each bone.

Coronomeckelians (Fig. 6C: *sa*) These are small chips anteromediad to the endosteal process and covered by Meckel's cartilage. Starks (1916) presents a brief description of this bone, termed sesamoid articular, for related pleuronectids.

Premaxillaries (Figs. 1; 6A,B: *pmx*) The paired premaxillaries are the anteriormost dermal elements of the branchiocranium. Each fragile bone arcs anteromedially to meet the symphysis. The right element is anterior and ventral to the left. Bordering the symphysis are two thin vertical keels that extend their ensiform ascending processes dorsally to a point just above the maxillary head. A broad sheet of ligament (superficial ligament) extends from these processes to the prefrontals. The premaxillary-lateral ethmoid ligament, underlying the superficial tissue, extends to the left lateral ethmoid from the ascending processes of both premaxillaries. The shaft of each bone is supported by the overlying maxillary processes. The tricornered maxillary base is V-shaped to accommodate the anteromedial premaxillary flange. Canine teeth of uniform height line the ventromedial surface. The ramus of the left premaxillary is one-third longer than the right, conforming with the similarly proportioned dentaries.

Maxillaries (Figs. 1; 6A,B: *mx*) These dermal elements are situated above the premaxillaries. The right is anterior and ventral to the left. Each element is comprised of a long horizontal shaft with expanded anterior and posterior processes. The posterior labial limb terminates in a deltoid process (postmaxillary process of Yazdani, 1969), arising dorsomesially and ventromesially and is supported by the mandibulo-maxillary ligament passing from the inner ventral surface to the coronoid process of the dentary. The tricornered anterior expansion articulates with the autopalatine dorsally (cranial condyle) and the premaxillary ventrally (premaxillary condyles). The bulbous cranial condyle pivots against the prevomer. Anterior to this condyle is a broad, flat face bearing a low profile spike (maxillary spike). This prominence extends anteriomedially to meet a similar projection on its confrere. Posterolateral to the expansion is the retroarticular-maxillary ligament. The maxillary-ethmoid ligament extends to the ethmoid from a point below the cranial condyle of the right maxillary. The latter ligament together with the autopalatine-premaxillary

form the "crossed ligaments" and are present only on the right side. The two basal corners of the maxillary are separated by an intervening V-shaped depression. The premaxillary flange articulates within the depression restricting lateral and distal dislocation of the premaxillary. The left maxillary is about one-eighth longer than the right and both flank their premaxillaries posterolaterally.

Hyoid Region

This region is comprised of nine paired elements plus eight paired branchiostegal rays and two uniserial bones, the basihyal and the urohyal. Only six of the paired elements are cartilage bones: hyomandibulars, interhyals, epihyals, ceratohyals, upper hypohyals, lower hypohyals. The other three are of dermal origin: interoperculars, subopercular, and the opercular.

Hyomandibulars (Figs. 1; 5A,B: *hyo*) Each Y-shaped bone fits above into a fossa on the prootic-autosphenotic and the facet on the autopterotic. The left hyomandibular contacts the metapterygoid anteriorly via a thin winglike extension of its vertical shaft. The symplectic and interhyals contact each hyomandibular shaft ventromesially within a grooved recess of the overlying preopercular. A lateral blade traverses the hyomandibular to articulate within the anteriomesial groove on the preopercular. Between the opercular and autosphenotic process is an arched web of bone that acts as a rocker in hyomandibular movement.

A dorsomesial foramen marks the entrance of the hyomandibular branch of the facial nerve. The nerve exits midway down the hyomandibular shaft posterolaterally. The left bone differs from the right in two respects: 1) a low-profile strut supports the rocker web, and 2) the flange adjoining the metapterygoid has a linear margin, whereas the contralateral member is distinctly emarginate.

Interhyal (Fig. 7: *ih*) Each small subfusiform element is ligamentously attached dorsally to the hyomandibular shaft terminus and ventrally to the epihyal. The bone links the suspensorium to lower hyal elements.

Epihyal (Fig. 7: *eh*) These paired bones appear broadly lunate. Each has a pisiform process posterodorsally articulating with the interhyal above. Four branchiostegals are attached to each bone's ventral margin. Nelson (1969), among others, has pointed out that the epihyals are serial homologues of the epibranchials and therefore do not support branchiostegal rays. However, in keeping with the usage of Harrington (1955), the term epihyal is herein retained.

Ceratohyals (Fig. 7: *ch*) Each ceratohyal is sutured to the epihyal posteriorly, the upper and lower hypohyals anteriorly. A posteriorly directed serrated process overlies a portion of the epihyal. In lateral aspect, the bone narrows centrally and widens again anteriorly. A broad anteroventral excavation supports the remaining four branchiostegals.

Upper hypohyals (Fig. 7: *uhh*) These small tetrahedral elements are sutured to their ceratohyals posteriorly and lower hypohyals ventrally. Each upper hypohyal angles medially articulating with the first basibranchial.

Lower hypohyals (Figs. 1, 7: *lhh*) Each small triangulate bone caps the anterioventral portion of the hyal complex and is strongly sutured to the upper hypohyal and ceratohyal. The two meet in midsagittal plane.

Basihyal (Figs. 1, 7: *bh*) This horizontal cylindrical element supports the tongue anteriomedially. The bone is wedged within cartilage at the dorsomedial convergence of the upper hypohyals. According to Nelson (1969), this bone represents three copulae.

Urohyal (Fig. 7: *urh*) Situated under the basibranchials and surrounded by the hyoid arch, this element supports coracohyoid musculature in sagittal plane. The rostral process (Fig. 7: *r*) projects anteriorly with its apex abutting the upper-lower hypohyal suture. Posteriorly, the dorsal shank forks; the left prong is slightly longer than the right one.

A thin translucent plate is directed ventrally and tapers to an emarginate blade.

Branchiostegals (Figs. 1, 7: *b*) There are eight pairs of branchiostegal rays, four based on the ventral margin of the epihyals and four attached to the ceratohyals. Each cylindrical bone curves laterally and ventromedially to terminate in a needle point. A connective membrane extends across the branchiostegals and is attached to the interopercular margin laterally and subopercular margin posterolaterally.

Interoperculars (Fig. 1: *iop*) Each translucent dermal element is ventral to the preopercular and its horizontal dorsal margin locks into a ventromesial preopercular furrow. Its posterodorsal apex overlaps the anterior margin of the subopercular.

Suboperculars (Fig. 1: *sop*) Each thin convex element is bound by membrane to the opercular and interopercular. The ventral margin of each supports the branchiostegal membrane. A lobe of the opercular overlies each anterodorsally.

Operculars (Fig. 1: *op*) These broad triangular dermal bones possess condylar dorsal apices which articulate with the posterodorsal hyomandibular extensions. Two convex ridges traverse each bone from the dorsal condyle posteroventrally to each bone's trenchant margin. Each element tapers ventrally to a thin translucent cartilage coplanar with the subopercular. The adductor operculi inserts dorsomedially after originating on the autopterotic limb. No foramina pierce these bones.

Branchial Region

This region is dorsomediad to the hyoid region and consists of the following endochondral bones: four pairs of pharyngobranchials, four pairs of epibranchials, five pairs of ceratobranchials, three pairs of hypobranchials, three basibranchials. The gill rakers are dermal in origin. These five arches support the respiratory musculature, gills and pharyngeal teeth. Each arch surrounds the branchial cavity.

The descriptive terminology follows that of Topp and Cole (1968): proximal and distal are used with respect to the neurocranium; abpharyngeal and adpharyngeal position of the bones relative to the pharyngeal cavity.

Basibranchials (Fig. 8: *bb1, bb2, bb3*) These three unpaired medial elements (copulae) lie in connective tissue and comprise the floor of the pharyngeal cavity. The first triangulate basibranchial contacts the upper hypohyals at their median symphysis; the second hourglass shaped ossification is distal to the first basibranchial, and is flanked proximally and distally by two pairs of hypobranchials and respectively. The latter hypobranchial pair barely contacts the central basibranchial, but converges along two-thirds the border of the triangulate third basibranchial. A single median cartilage extending distally represents two nonindependent basibranchials (Nelson, 1969). From the abpharyngeal fac e of the second basibranchial arises a Y ridge; the two legs articulate with short spinous processes projecting from the abpharyngeal proximal edge of the hypobranchials.

Hypobranchials (Fig. 8: *hb1, hb2, hb3*) The three paired hypobranchials flank the basibranchials laterally. These elements also lie in connective tissue and complete the floor of the branchial cavity. The curved splintlike first hypobranchial pair articulates distally with the second basibranchial and they articulate with the first ceratobranchials dorsolaterally. Each bone supports a single gill raker. The rhomboidal second hypobranchials contact the third basibranchial adpharyngeally and the second basibranchial abpharyngeally. Two gill rakers are supported on each bone's margin. The spatulate third hypobranchials contact the abpharyngeal surfaces of the third basibranchial and second hypobranchials at their symphysis.

Ceratobranchials (Fig. 8: *cb1–cb5*) Four of

these slender rods constitute the primary supporting elements of the gills abpharyngeally and the gill rakers adpharyngeally ("lower limbs"). The first three ceratobranchials contact their respective hypobranchials ventromedially and epibranchials dorsomedially. The fourth pair are cartilaginously attached to the third ceratobranchials and third hypobranchials. The fifth pair supports only the conical teeth on their adpharyngeal surface. Each semilunate bone terminates distally in a blade.

Epibranchials (Fig. 8: *eb1–eb4*) Two of the four epibranchial pairs differ in form but all articulate dorsally with their respective pharyngobranchials and ventrally with their ceratobranchials. The first two splintlike epibranchials support gill rakers on their adpharyngeal surfaces ("upper limbs"). The first element is only slightly broader and longer than the second. The third element is heavier and nearly Y-shaped. This bone supports two gill rakers on its adpharyngeal margin. According to Branson (1966), the levator arcuum branchialium is inserted in the vertical mediad process. The last epibranchial angles mediad to abut the bony web of the third epibranchial just below its vertical process. Tooth plates are not fused to the epibranchials as in more primitive species of fishes (Nelson, 1969).

Pharyngobranchials (Fig. 8: *pb1–pb4*) The first splintlike toothless pharyngobranchial extends proximally and laterally contacting the prootic anterior to the otic capsule. The bone overlies the heavy musculature supporting the remaining elements bearing conical teeth. The musculature is supported by the opisthotic and basioccipital.

The second arcuate pharyngobranchial is the largest of the series and bears three rows of curved conical teeth on its adpharyngeal margin. The supporting concave bone abuts the third pharyngobranchial, which is also arcuate but bears a single row of teeth. The last pharyngeobranchial is strongly concave in posterior view and supports a single row of villiform teeth. Each element is nestled in the concavity of its proximal associate. The pharyngobranchials are supported by both the third and fourth epibranchials.

Gill rakers (Fig. 8: *g*) The gill rakers form a single series on the epi-, cerato-, and hypobranchials of the first two arches and on the epi- and ceratobranchials of the third arch. The fourth ceratobranchials maintain a double row of gill rakers (inner and outer) on their adpharyngeal margins. The lower limb (ceratobranchial) supports eight rakers and from nine to ten, including the first and second hypobranchials, respectively. Norman (1934) states that the lower part of the anterior arch supports from nine to twelve gill rakers. The number on the lower first arch did not vary in all specimens examined.

Vertebral Column

Specimens taken from the Georges Banks area had 46 vertebrae, wheras those captured in waters off Gloucester had 47 vertebrae. Above each amphicoelous centrum is a neural arch which supports a spine; from each foot of the arch arise the neural zygapophyses. All vertebral bones are endochondral in origin: 12–14 trunk vertebrae; 32–34 caudal vertebrae, including the terminal vertebra (Fig. 13: *tv*), the penultimate vertebra (Fig. 13: *pv*), the antepenultimate vertebra (Fig. 13: *apv*), 8–10 pairs of pleural ribs, 10–12 pairs of epipleural ribs. Although the numbers of trunk and caudal vertebrae vary by three elements, the total number only varies by two. Thus a predictable numerical relationship apparently exists between the two portions of the vertebral column. For example, a specimen with 14 trunk vertebrae would normally possess 32 or 33 caudal vertebrae.

Each cylindrical centrum bears horizontal supporting ridges with numerous blind canals. Dorsomedially, the neural arch encases the central nerve cord and is pierced laterally by two paired foramina for the passage of nerve fibers to the dorsal and ventral horns of the cord. The foramina vary, but are commonly lacking in the first two and last ten vertebrae. These fibers pass dorsally and ven-

trally over the centrum ridges along their respective neural and haemal spines.

A ventromedial haemal arch encases the caudal artery and bears a single pair of foramina for the passage of vessels to the hypaxial and epaxial muscle masses. Excluding the terminal vertebra, all caudal vertebrae bear haemal and neural processes, but lateral foramina are generally excluded from the first 4 and last 4 caudal vertebrae. In several vertebrae (numbers 18–21) haemal foramina may be either closed or poorly developed. Lateral apophyses appear on the right side of one or more vertebrae (numbers 11–16). These processes appear equally distributed among males and females. The primary function of lateral apophyses is for muscular support, and according to Ford (1937), in *H. platessoides* they are primarily found on the caudal vertebrae of the eyed side. In several specimens, however, the most prominent lateral apophysis was found on the centrum of the last trunk vertebra. The presence of these projections adds to the asymmetry of the centra.

The median skeletogenous myoseptum is attached to the spines within grooves situated on the anterior and posterior surfaces. The proximal pterygiophores are situated within the interspinous myosepta. Two proximal pterygiophores are frequently bound by ligament to each spine anteriorly and posteriorly in median plane, but there are several exceptions: 8–10 proximal pterygiophores are attached directly to the supraoccipital crest and left frontal, three have coalesced on the interhaemal spine ventromedially, 5–8 others are bound to the interhaemal spine and the second caudal vertebra posteriorly. The 10 to 14 proximal pterygiophores contributing to the posteriormost portion of the median fins do no appear to be associated with the spines.

Neural spines (Figs. 10A, 11, 13: *ns*) are nearly perpendicular to the vertebral axis in the trunk region. Beginning with the second caudal vertebra both neural and haemal spines incline posteriorly, the angle with the vertebral axis becoming less obtuse (approximately 30°) to the axis at the penultimate vertebra.

Beginning at vertebra 27 and extending through vertebra 32, the vertebral axis twists counterclockwise, the final posterior plane no more than 10° removed from the anterior plane. A similar twist occurs in the spinal column of *Psettodes erumei* and perhaps several pleuronectids but accounts of this phenomenon are lacking (Kirtisinghe, 1937).

Trunk vertebrae (Figs. 9; 10) There are from 12 to 14 trunk vertebrae, the larger number found in specimens from cold waters. All possess a neural process and lack a haemal spine. The neural spine of the atlas (vertebra 1) has a basal arch ankylosed with both first and second centra, thereby rendering the latter two immovable. Its spine projects well above the level of the cranium. Each vertebra, except the atlas, supports ventrolateral parapophyses, which become successively longer and broader posteriorly. In lateral aspect parapophyses are broadly triangulate. An anterior vertical ridge traverses each parapophysis (Fig. 10A: *par*) from the centrum to the apex and is immediately followed by a vertical posterior furrow. Lateral depressions at the apices receive the epipleural ribs.

Each vertebra bears neural prezygapophyses (Figs. 10A,11: *nprz*) and neural postzygapophyses (Fig. 10A: *npoz*) for articulation with its associates. In all trunk vertebrae except the atlas that maintains two dorsolateral condyles, prezygapophyses are substantial and in vertebrae 2 to 5 extend well onto the preceding vertebra.

One or more centra in the region of vertebrae 11 to 13 commonly support lateral apophyses (Fig. 11: *epp*). This process is generally located at the right lateral surface where the parapophysis joins the centrum.

Vertebra 3 (Fig. 10A). This vertebra is marked by pyramidal parapophyses notched terminally for the second epipleural rib. The pre-

zygapophyses project onto the centrum of the second vertebra. The concave centrum is dorsoventrally compressed.

Vertebra 4 (Fig. 10A). This cylindrical vertebra also possesses monolithic parapophyses notched to accommodate the epipleural ribs. The neural postzygapophyses possess broad lateral faces.

Pleural ribs (Fig. 9: *pr*) The number of ribs varies with the trunk vertebrae count and side under examination. In specimens with 14 trunk vertebrae there are 11 right pleural ribs (vertebrae 3–13) and 10 left ribs (vertebrae 4–13). Those specimens with 13 trunk vertebrae have one fewer rib on each side. In two additional specimens, bisymmetry in number of pleural and epipleural ribs is evident. The slightly expanded basal portion of each rib articulates with the parapophysis posterolaterally, while their needlelike shafts are directed ventrally at approximately 60° to the vertebral axis. Each rib becomes successively longer and more lunate excluding the two posteriomost elements.

Epipleural ribs (Fig. 9: *epr*) The number of needlelike epipleural ribs also varies with the number of trunk vertebrae and side under examination. Specimens with 14 trunk vertebrae possess 13 right elements (vertebrae 2–14) and 12 left elements (vertebrae 2–13). The longest epipleurals are located anteriorly.

Caudal vertebrae (Figs. 9; 10A; 11) Aside from the first five caudal vertebrae which possess laterally expanded haemal spines and the conical terminal vertebra, the 26 to 28 remaining vertebrae are persistently uniform except for their decreasing diameter with each posterior element.

With the exception of the first two caudal vertebrae, the neural prezygapophyses and neural postzygapophyses have no equivalent articulating surfaces on bases of haemal spines. The primary support for each biconcave centrum, therefore, remains on the discoid dorsoventrally flattened perimeter.

The haemal spines (Figs. 10A, 11, 13: *hs*) are about 20% longer than the neural spines. Their anterior-posterior grooved surfaces support the median skeletogenous myoseptum.

The first caudal vertebra possesses the longest of the spine series. The haemal spine maintains wide lateral flanges spanning its length. A supporting tubular canal underlies the deep groove ventrally and extends from the apex to end blindly in the bone's midportion. This haemal spine, in turn, supports the interhaemal spine, which protects the ventral margins of the body cavity and terminates anteroventrally in a strong point commonly considered a spinous ray.

Median Fins

Both dorsal and anal fins traverse the length of the body. The former originates on the neurocranium (left frontal) dorsal to the eye and extends to the caudal peduncle, whereas the latter originates behind the vent but also extends to the caudal peduncle. There are no spinous ray supports, although some consider the terminus of the interhaemal spine a fin structure. In addition to the rays, the supporting structure includes a tripartite system; the proximal pterygiophores that interdigitate with the neural and haemal spines, the intermediate pterygiophores and the distal pterygiophores.

Dorsal fin (Fig. 9) The cartilage bones are: 88–91 proximal pterygiophores, 88–91 intermediate pterygiophores, 88–91 distal pterygiophores. The dermal bones consist of 88 to 91 lepidotrichs.

Anal fin (Figs. 9, 10, 11) The tripartite elements supporting the 68 to 71 dermal lepidotrichs are the 65 to 68 endochondral, proximal pterygiophores, the 66 to 69 intermediate pterygiophores, and the 68 to 71 distal pterygiophores. Three proximal pterygiophores and two intermediate pterygiophores are fused with the interhaemal spine. (Fig. 9: *ihs*).

Pterygiophores (Figs. 9;10 B: *ppt, ipt, dpt*) The proximal pterygiophore consists of a long tubular shaft tapering distally into four keels each juxtaposed 90° to its neighbor. The coplanar medial keel becomes less prominent with each posterior element but remains colinear with the intermediate pterygiophores. Erector and depressor muscles originate on these bladelike projections.

Each intermediate pterygiophore is ankylosed to an adjoining proximal pterygiophore. The former triangulate bone retains two (anterior-posterior) cuplike depressions supporting the distal pterygiophore through a complement of intervening cartilage. The grooved lateral surfaces are colinear with the winged processes of the proximal pterygiophore.

Distal pterygiophores are recessed within the base of each lepidotrich but extend medially to contact the cuplike fossa on each intermediate pterygiophore pair. These were present within all lepidotrich bases.

Appendicular Skeleton

Pectoral Girdle and Fin

The girdle- and fin-supporting structures consist of five paired and two unpaired elements. The cartilage bones are: coracoids, scapulars, actinosts. The dermal bones are: cleithra, supracleithra, postcleithra, and the lepidotrichs. Each girdle arch is ligamentously attached to the posttemporal of the neurocranium.

Supracleithra (Figs. 1,12A,B: *scl*) Each flat hastate element flanks the cleithrum posterolaterally and contacts the posttemporal anteromesially. Their lateral surfaces are free from laterosensory canals though their dorsoposterior margins are somewhat cancellous.

Cleithra (Figs. 1,12A,B: *cl*) These are the longest bones of the pectoral girdle and provide the primary support for the remaining elements. The anterodorsal margin and anteromesial face are contacted by the supracleithra. Ventral to the supracleithrum each bone forms an obtuse angle, the distal arm about 100° to the proximal arm. The coracoid, scapula, and postcleithrum fit neatly into a mesial recess on each bone's curvature. A V-shaped lateral groove traverses the distal limb of both bones.

Postcleithra (Figs. 1,12A,B: *pcl*) These paired cylindrical bones are attached to the dorsomesial flexure of the cleithrum. Each thin lunate element is reinforced by a dorsal ridge. A spike of bone arising from each element's dorsomedial curvature extends posteriorly. Contact with the scapula and coracoid is denied by a sheet of intervening tissue.

Scapulae (Figs. 1,12A,B: *sc*) These thin, flat triangulate bones are ligamentously bound to the mesially grooved cleithra. The left element is slightly larger than the right. Each supports two actinosts on their posterior margin. The bones are coplanar with the coracoid ventrally.

Coracoids (Figs. 1,12A,B: *cor*) Each thin, bifid element is bordered dorsally by the scapula, but the right element differs from the left in that its ventral process contacts the cleithrum. Two actinosts are imbedded in cartilage posteriorly.

Actinosts (Figs. 1,12A,B: *ac*) There are four pairs of styloid actinosts, two supported by each scapula and two others lying posterior to each coracoid. The ossified portion of these latter two elements appears cylindrical and laterally flattened. Those lying posterior to the scapula are fused in older specimens and only their centers are ossified; all are lodged in cartilage and are graded in size, the dorsalmost element being the smallest.

Lepidotrichs (Figs. 1,12A,B) Eleven paired lepidotrichs comprise the pectoral fin-supporting elements. Eight lepidotrichs articulate with the actinosts and three with the scapula.

Pelvic Girdle and Fin

This girdle consists of the paired endochondral basipterygia and the dermal lepidotrichs.

Basipterygia (Figs. 1,12C: *bpt*) These two triangular elements are apposed mesially to form the girdle. Each possesses a bony ridge along its posterodorsal margin and a bladelike anteroventral keel. The anterior apex of each element is ligamentously bound to the cleithrum mesially.

Lepidotrichs (Fig. 12C) Six paired lepidotrichs articulate with each basipterygium ventrally.

Caudal Skeleton

Synonymy of the caudal skeleton is based on the works of Gosline (1961), Monod (1968), and Rosen and Patterson (1969). Although Whitehouse (1910) and Barrington (1937) have provided detailed descriptions of *Solea lutea* and *Pleuronectes platessa* caudal skeletons, respectively, terminology used by these investigators differs. The pleuronectid caudal skeleton is a highly specialized perciform derivative. In *H. platessoides* two triangulate hypural plates replace six hypurals, urostyle and uroneurals of percoid forms. The anteriormost epural has been incorporated in the penultimate neural spine leaving two epural elements (Rosen and Patterson, 1969). A single ventral parhypural is free from the terminal vertebra. Monod (1968) designates the former bone a hypural when two epurals exist above, but this is not the case in *H. platessoides*. In small specimens the first hypural plate is autogenous and possesses a rudimentary flange which disappears as the plate fuses with the terminal vertebra (Fig. 13: *tv*). The two epurals by definition (Gosline, 1961) are free of the terminal centrum and support caudal fin rays distally. Haemal spines anterior to the terminal vertebra are sessile in specimens greater than 244 mm standard length (SL) although in at least one specimen of 172 mm SL a partial suture appears at the base of the first anterior spine.

Parhypural (Fig. 13: *phu*) This single triangular element is wedged between the first hypural plate and the haemal spine of the penultimate vertebra (Fig. 13: *pv*). At an early stage its proximal apex is free from the terminal vertebra and projects anteriorly within the margins of the haemal spine but is fused at the spine's base in specimens over 778 mmSL. This is equivalent to Hypural 1 of Gosline (1961).

Hypural plates (Fig. 13: *hu1–2*) The first broad triangular plate possesses a ventrolateral flange that disappears with age. In young specimens the plate contacts the terminal vertebra but is fused with the latter element in mature animals. The second plate, also triangulate, remains inseparably fused to ther terminal vertebra. The urostylar and uroneural elements appear to have been incorporated in the plate during ontogenetic development, although the exact dispostion of the uroneurals remains open for discussion. Since the perciform ancestor has six hypurals (Gosline, 1961), the first hypural plate probably represents the fusion of two such elements; the second hypural plate represents three fused elements.

Epurals (Fig. 13: *eu1–2*) The splenoidal second epural lies dorsal to the second hypural plate with its proximal border free from the terminal centrum. The first splintlike element is enveloped by the neural process of the penultimate vertebra. Unlike the parhypural its base does not fuse with the spine. The perciform ancestor possesses three epurals and examination of young specimens further substantiates the hypothesis set forth by Rosen and Patterson (1969) that the dorsal-most epural has been incorporated in the neural spine of the penultimate vertebra.

Lepidotrichs (Fig. 13) There are 18 branched lepidotrichs: four supported by the parhypural, five by the first hypural plate, six by the second hypural plate, two by the second epural and one on the first epural.

Acknowledgments

Critical comments of Mr. Robert W. Topp, Mr. Charles R. Futch, and Mr. Andrew Konnerth are gratefully acknowledged. We also wish to thank Mr. Paul J. Godfrey for his valuable suggestions. Additional specimens were provided by Mr. Peter K. Prybot and Dr. Marvin Grosslein.

Time to complete this project was being provided to the senior author before his death by the Middle Atlantic Coastal Fisheries Center and by the Atlantic Estuarine Fisheries Center while he was in their employ. Subsequent to his death Dr. John B. Pearce and Mr. James E. Sykes of those Centers have been most helpful in providing assistance in funding the publication. The Massachusetts Cooperative Fishery Research Unit and the Zoology Department of the University of Massachusetts have also acted as sponsors and the help of Dr. Roger J. Reed and Dr. John D. Palmer are gratefully acknowledged.

Literature Cited

Barrington, E. J. W. 1937. Structure and development of the tail in the plaice *(Pleuronectes platessa)* and the cod *(Gadus morhua).* Quart. J. Microsc. Sci. (London), N.S., 79:447–469.

Bigelow, H. B., and **W. C. Schroeder.** 1953. Fishes of the Gulf of Maine. U.S. Fish and Wildl. Serv., Fish. Bull. 53:1–577.

Branson, B. A. 1966. Guide to the muscles of bony fishes, excluding some special fibers in the siluroids and a few others. Turtox News 44:98–102.

Chabanaud, P. 1933. Contribution a l'ostéologie comparative des poissons principalement des téléostéens Hétérosomes. Bull. Soc. Zool. Fr., 58:140–168.

———1934. Le complexe basiphénoidien et le septum orbitaire nadiral des Poissons Hétérosomes. C. R. Hebd. Séances Acad. Sci. [Paris] 198:1875–1877.

———1935. Le vomer, le complexe ethmoidien et le trajet periphérique des-
nerfs olfactifs des Téléostéens soleíformes. C. R. Acad. Sci. [Paris] 201:351–353.

———1936. Le neurocrane osseux des Téléostéens dyssmetriques après la metamorphose. Ann. Inst. Océanog. [Paris], N.S., 16:223–297.

———1938. Contribution à la morphologie et à la systematique des téléostéens dyssymetriques. Arch. Mus. His. Natur. [Paris] 6:59–139.

Cope, E. D. 1871. Contribution to the ichthyology of the Lesser Antilles. Trans. Amer. Phil. Soc. 14:445–483.

Evans, H. E. 1948. Clearing and staining small vertebrates *in toto,* for demonstrating ossification. Turtox News 26:42–47.

Ford, E. 1937. Vertebral variation in teleostean fishes. J. Mar. Biol. Assoc. U.K. 22:1–60.

Gill, T. 1864. Synopsis of the pleuronectoids of the eastern coast of North America. Proc. Acad. Natur. Sci., Philadelphia 16:214–224.

Gosline, W. A. 1961. The perciform caudal skeleton. Copeia 1961:265–270.

Gregory, W. K. 1933. Fish skulls: a study of the evolution of natural mechanisms. Trans. Amer. Philos. Soc. 23:75–481.

Harrington, R. W., Jr. 1955. The osteocranium of the American cyprinid fish, *Notropis bifrenatus,* with an annotated synonomy of teleost skull bones. Copeia 1955:267–290.

Hollister, G. 1937. Caudal skeleton of Bermuda shallow water fishes. II. Order Percomorphi, Suborder Percesoces: Atherinidae, Mugilidae, Sphyraenidae. Zoologica 22:265–279.

Jordan, D. S., and **B. W. Evermann.** 1898. The fishes of North and Middle America. Bull. U.S. Nat. Mus. 47 (Part 3):2614–2617.

Kirtisinghe, P. 1957. The vertebral column of the flatfish *Psettodes erumei* (Bloch and Schneider). Ceylon J. Sci., N.S. 1:67–72.

Konnerth, A. 1965. Preparation of ligamentary articulated fish skeletons. Curatory 8:325–332.

Kyle, H. M. 1921. The asymmetry, metamorphosis and origin of flatfishes. Phil. Trans. Roy. Soc. London, Ser. B. 211:75–129.

Lux. F. E. 1963. Identification of New England yellowtail flounder groups. U.S. Fish and Wildl. Serv., Fish. Bull. 63:1–10.

Lux, F. E., A. E. Peterson, Jr., and **R. F. Hutton.** 1970. Geographical variation in fin ray number in winter flounder, *Pseudopleuronectes americanus* (Walbaum), off Massachusetts. Trans. Amer. Fish. Soc. 99:483–488.

Monod, T. 1968. Le complexe urophore des poissons téléostéens. Mem. Inst. Fond. Afrique Noir. No. 81. 705 pp.

Nelson. G. 1969. Gill arches and the phylogeny of fishes with notes on the classification of vertebrates. Bull. Amer. Mus. Natur. Hist. 141:477–552.

Norden, C. R. 1961. Comparative osteology of representative salmonid fishes with particular reference to the grayling *(Thymallus arcticus)* and its phylogeny. J. Fish. Res. Bd. Canada 18:679–791.

Norman, J. R. 1934. A systematic monograph of the flatfishes (Heterosomata), Vol. I. Psettodidae, Bothidae, Pleuronectidae. Brit. Mus. (Natural History), London.

Regan, C. T. 1910. The anatomy and classification of the teleostean fishes of the Order Zeomorphi. Ann. Mag. Natur. Hist. 6:481–484.

Rosen, D. E., and **C. Patterson.** 1969. The structure and relationships of the paracanthopterygian fishes. Bull. Amer. Mus. Natur. Hist. 141:357–474.

Starks, E. C. 1916. The sesamoid articular: a bone in the mandible of fishes. Leland Stanford Junior Univ. Publ., Univ. Ser., Stanford Univ. Press. 40 p.

——— 1926. Bones of the ethmoid region of the fish skull. Stanford Univ. Publ. Univ. Ser., Biol. Sci. 4:139–338.

Taylor, W. R. 1967. Outline of a method of clearing tissues with pancreatic enzymes and staining bones of small vertebrates. Turtox News 45:308–309.

Topp, R. W., and **C. F. Cole.** 1968. An osteological study of the sciaenid genus *Sciaenops* Gill (Teleostei, Sciaenidae). Bull. Mar. Sci. 18:902–945.

Traquair, R. 1865. On the asymmetry of the Pleuronectidae, as elucidated by an examination of the skeleton in the Turbot, Halibut, and Plaice. Trans. Linn. Soc. 25:263–296.

Whitehouse, R. H. 1910. The caudal fin of the Teleostomi. Proc. Zool. Soc. London [1910]: 590–627.

Yazdani, G. M. 1969. adaptation in the jaws of flatfishes (Pleuronectiformes). J. Zool., London, 159: 181–222.

The Authors

David W. Frame. Dr. Frame died 8 September 1973. Part of his contribution to this work was done while he was on the staff of the U.S. Department of Commerce, National Marine Fisheries Service, Sandy Hook Laboratory, Highlands, New Jersey 07732. He completed it before his death while on the staff of the Atlantic Estuarine Fisheries Center, Beaufort, North Carolina 28516.

Thomas J. Andrews. Department of Zoology, University of Massachusetts, Amherst, Massachusetts 01003.

Charles F. Cole. Department of Forestry and Wildlife Management, University of Massachusetts, Amherst, Massachusetts 01003.

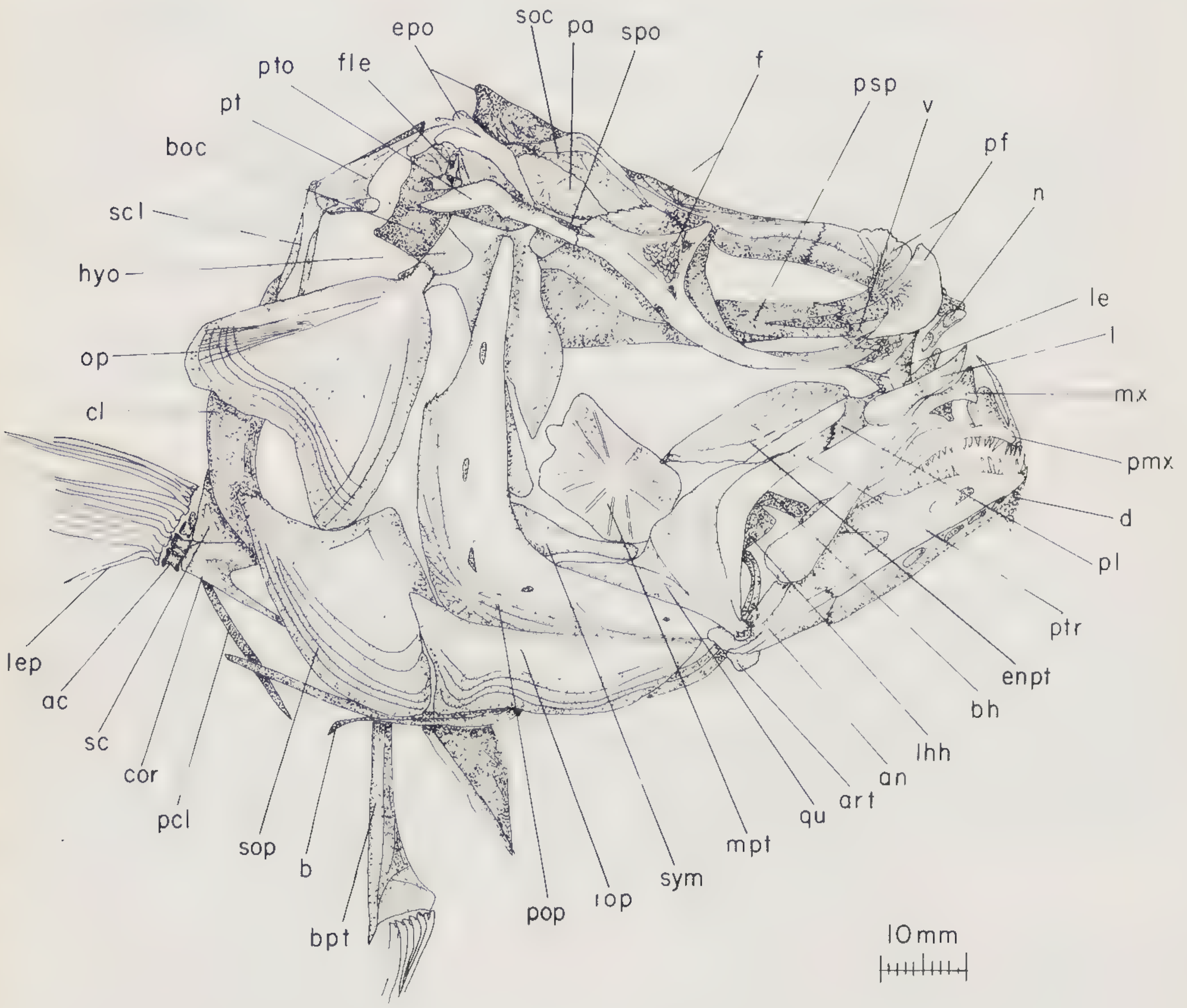

Fig. 1
Syncranium, skull length, 64 mm.

Fig. 2
Neurocranium, skull length, 68 mm: *A*) right side; *B*) ventral view; *C*) left side.

A

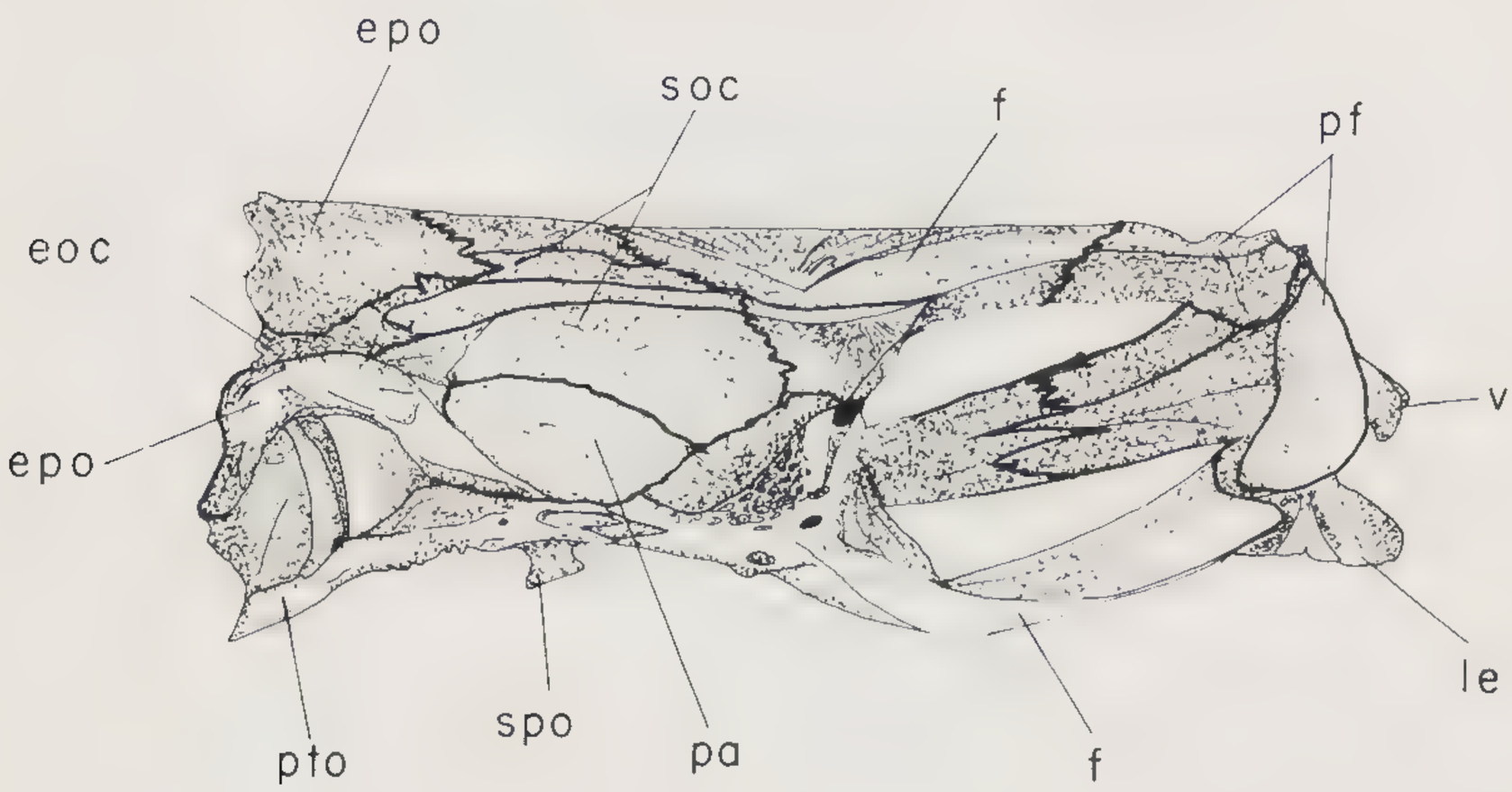
epo
soc
f
pf
eoc
v
epo
le
pto
spo
pa
f

B

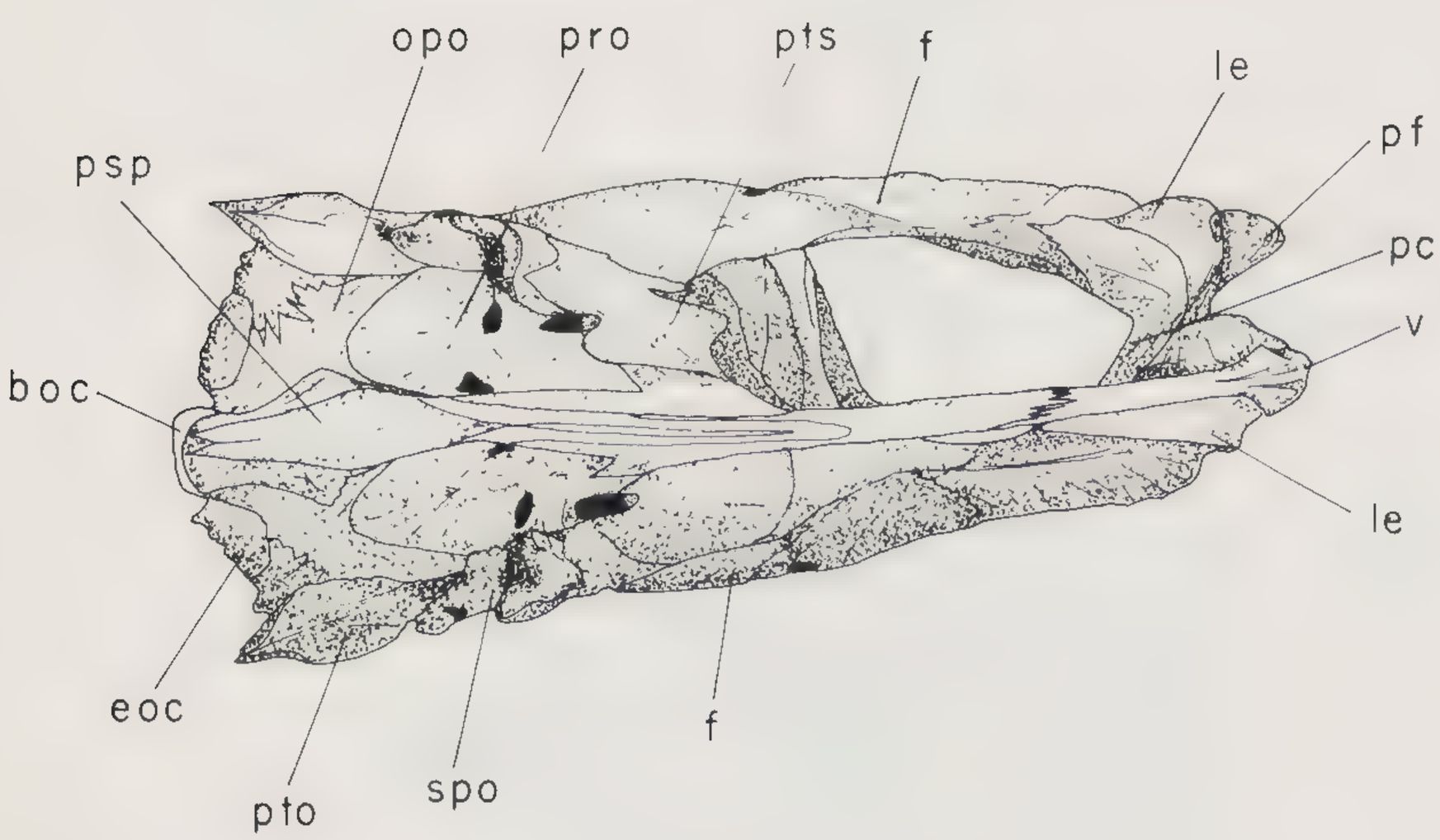
opo
pro
pts
f
le
pf
psp
pc
v
boc
le
eoc
f
pto
spo

C

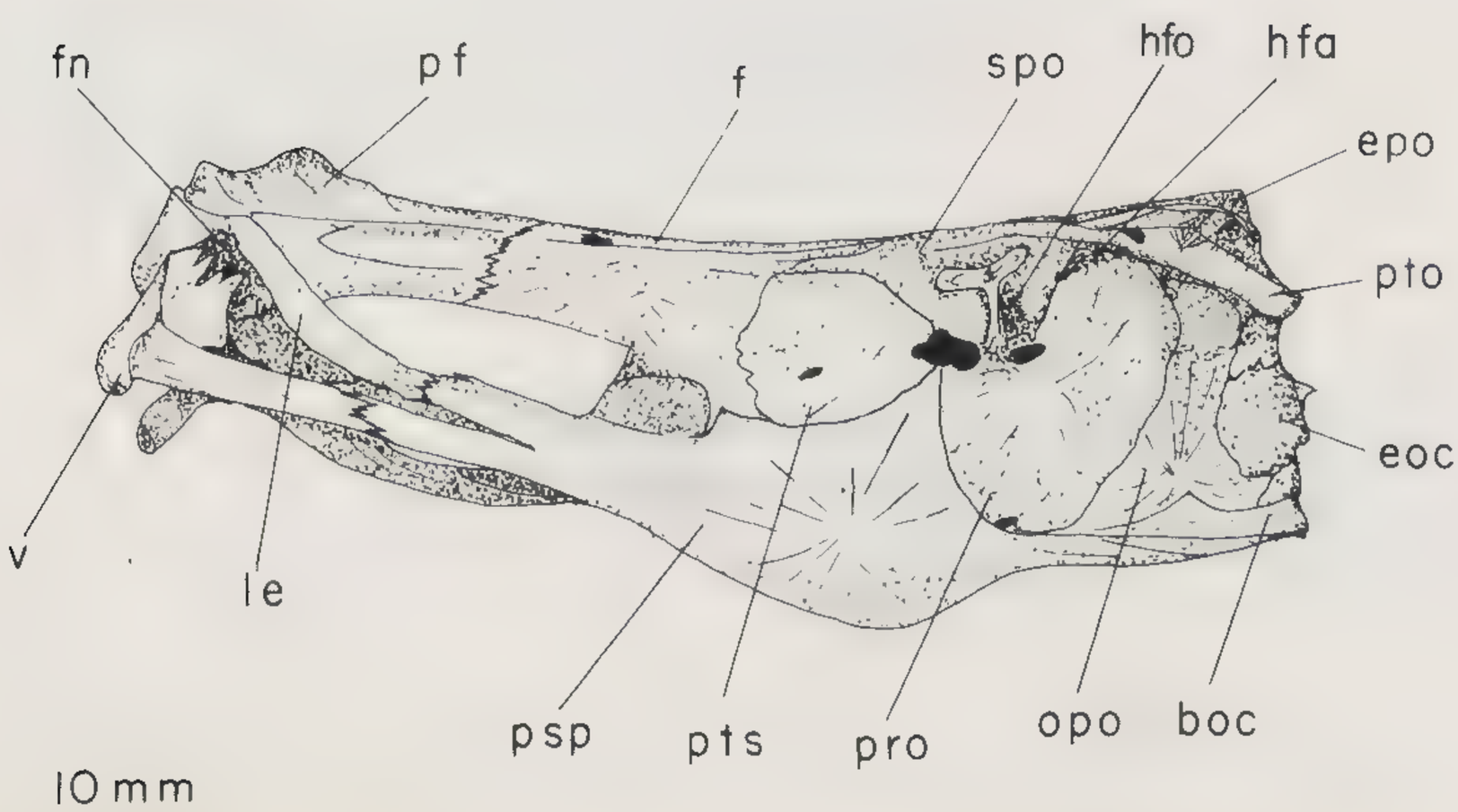
fn
pf
f
spo
hfo
hfa
epo
pto
eoc
v
le
psp
pts
pro
opo
boc
10 mm

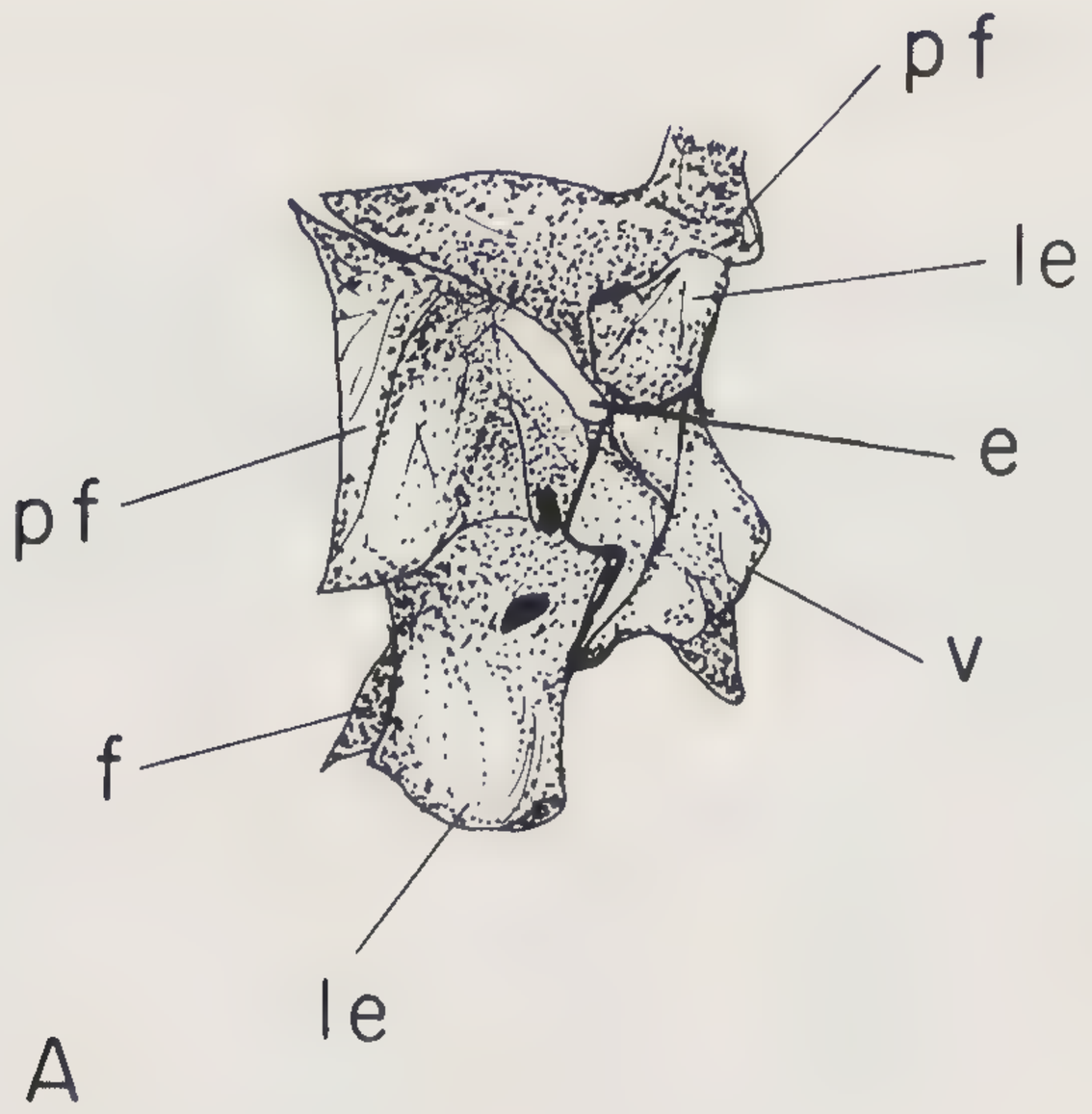

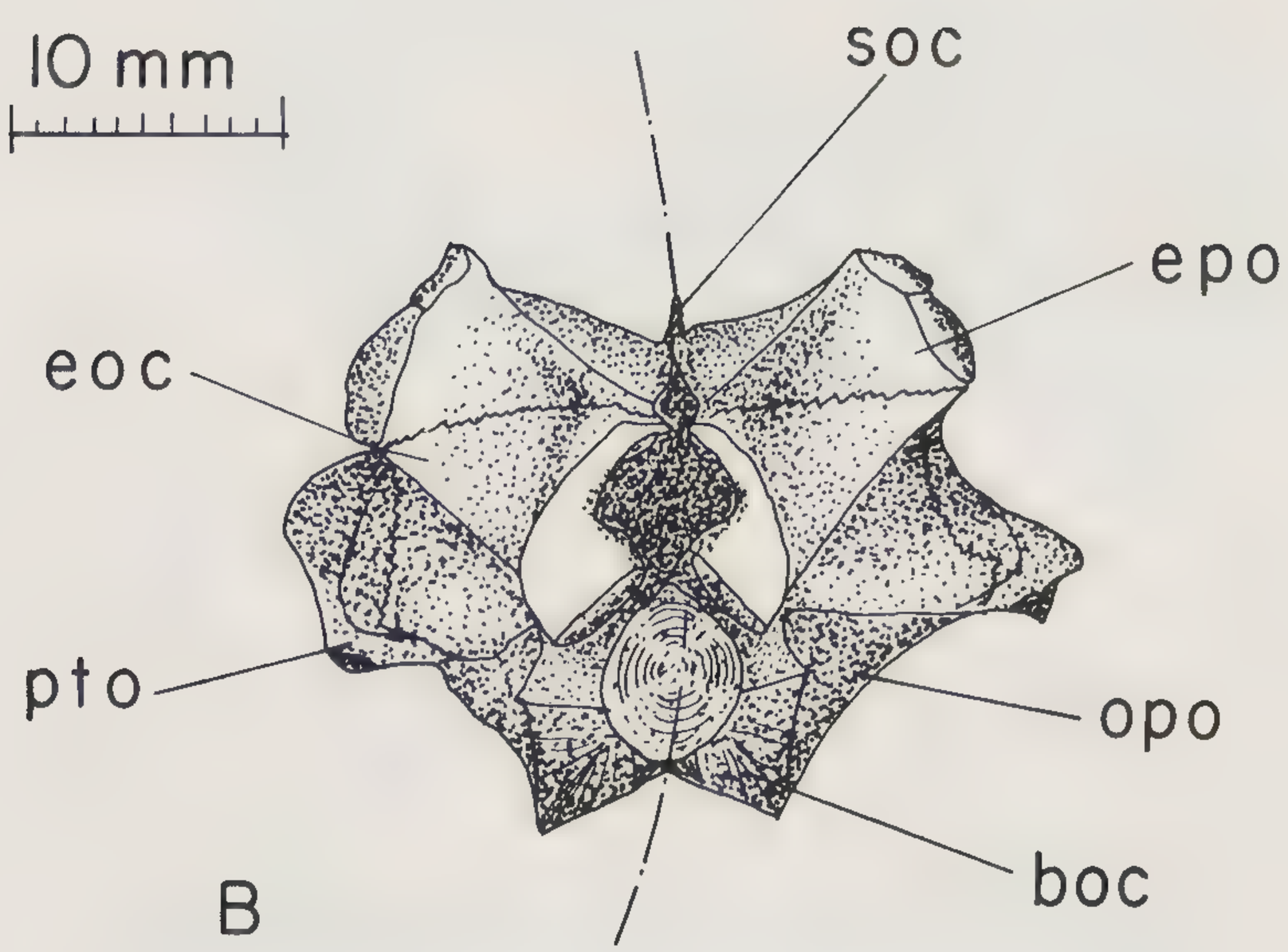

Fig. 3
Neurocranium, skull length, 68 mm: *A*) anterior view, olfactory region; *B*) posterior view, otic, occipital and basicranial regions.

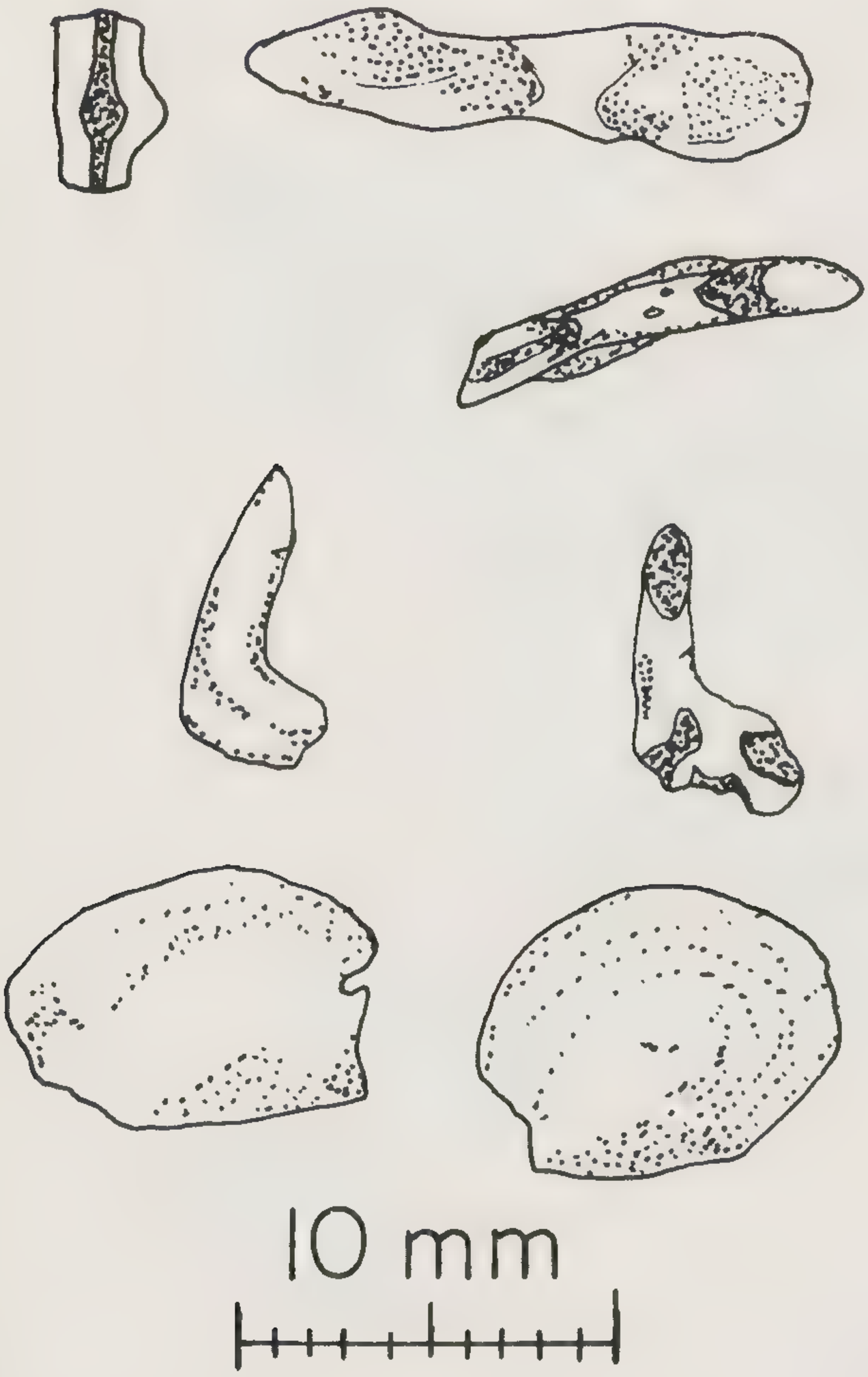

Fig. 4
Cranial elements from various specimens: first row, top (left to right) left and right lacrymals; second row: nasal; third row: median and lateral view of first lateral extrascapula; bottom row: ventral view of left and right otoliths.

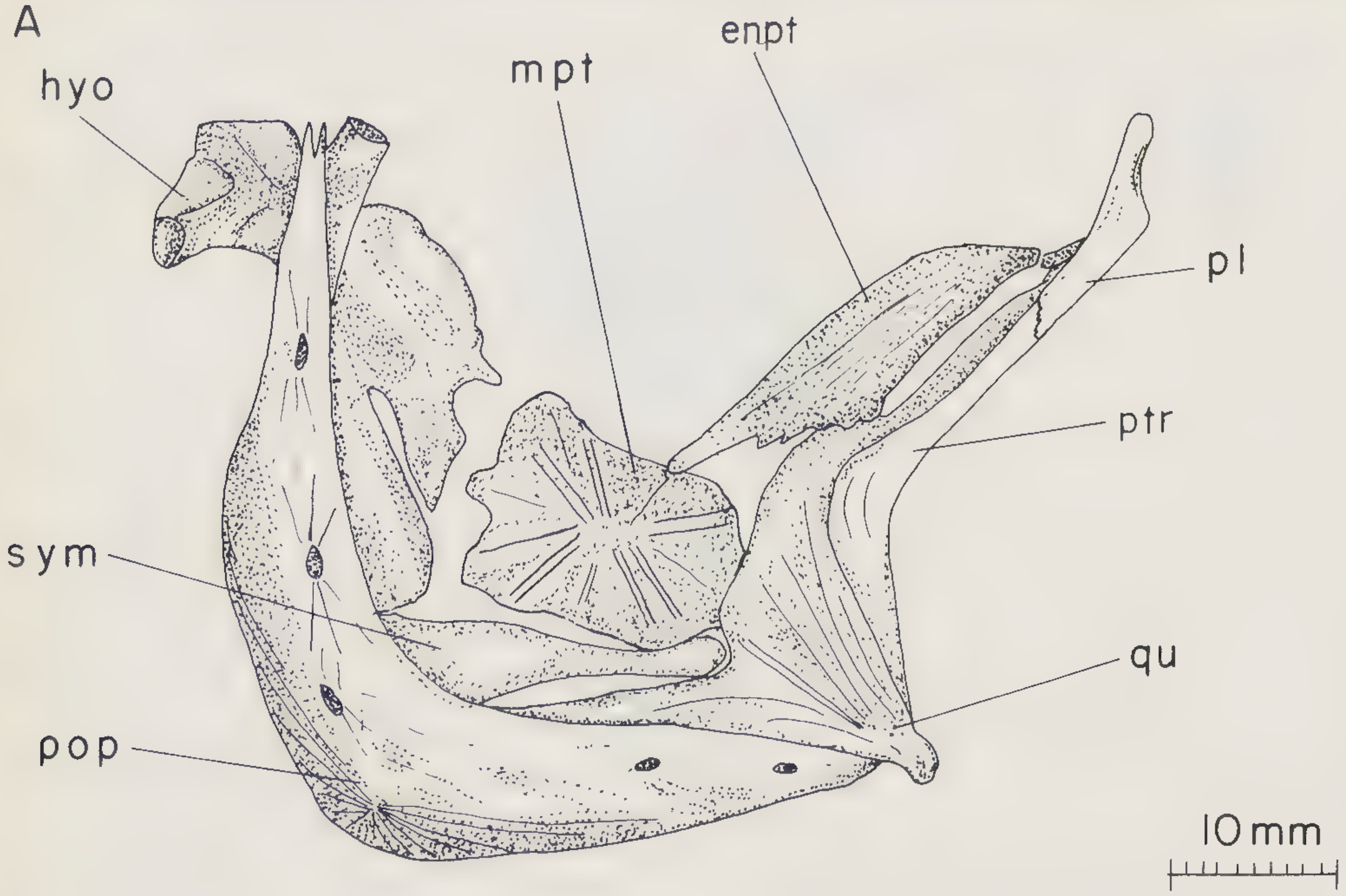

Fig. 5
Elements of the palatal complex and suspensorium prepared from Specimens 1 and 2: *A*) right side; *B*) left side.

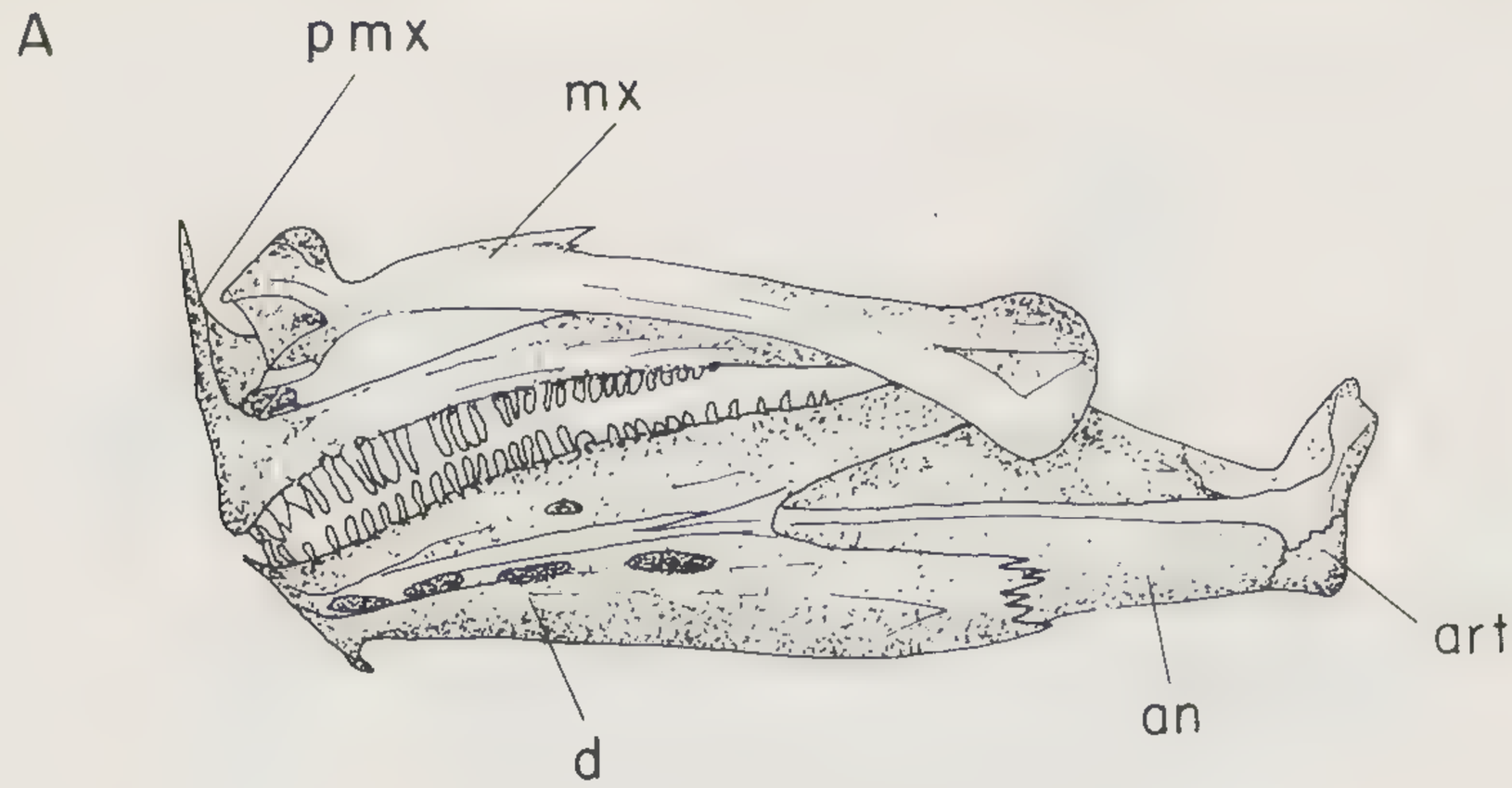

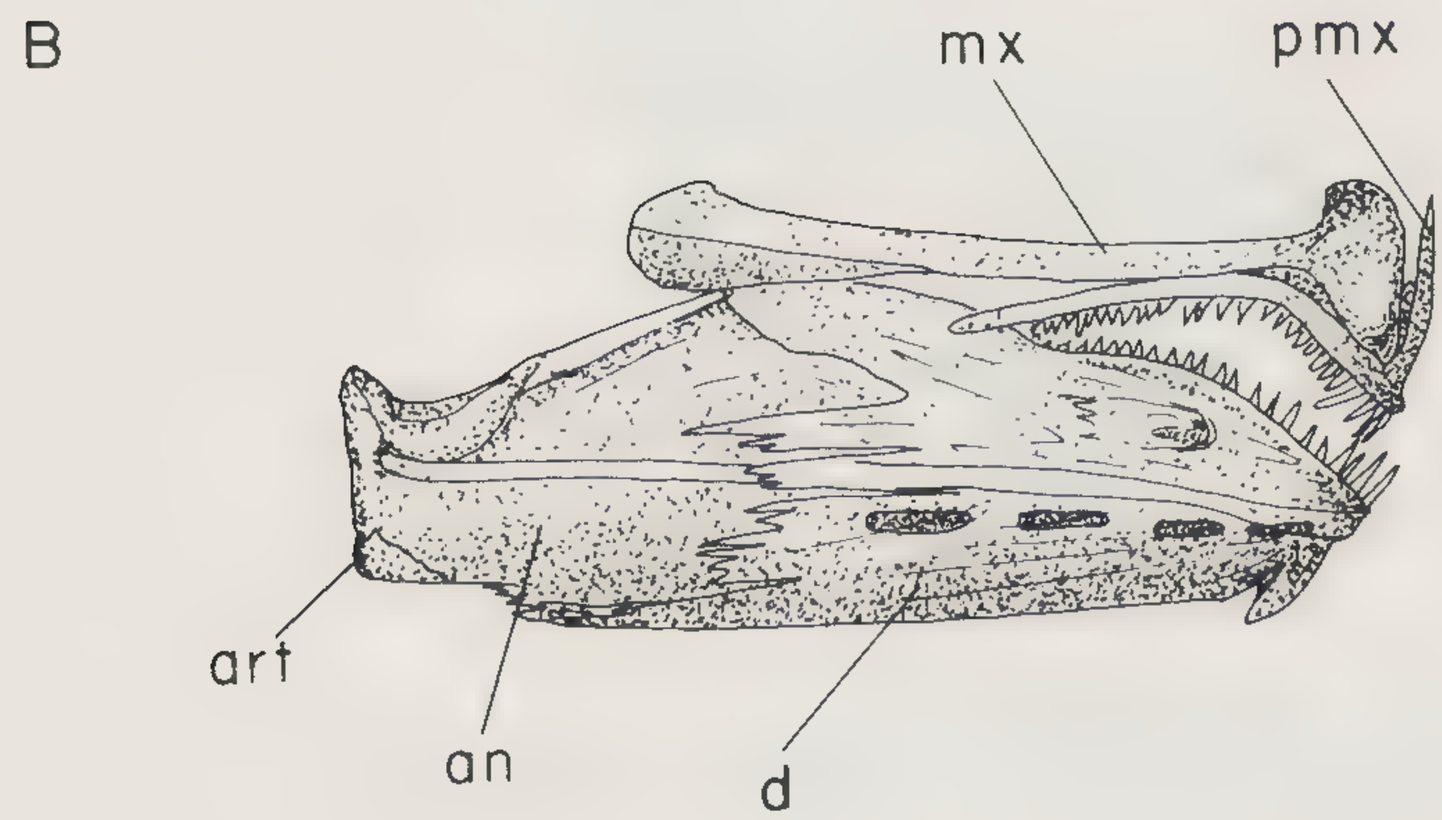

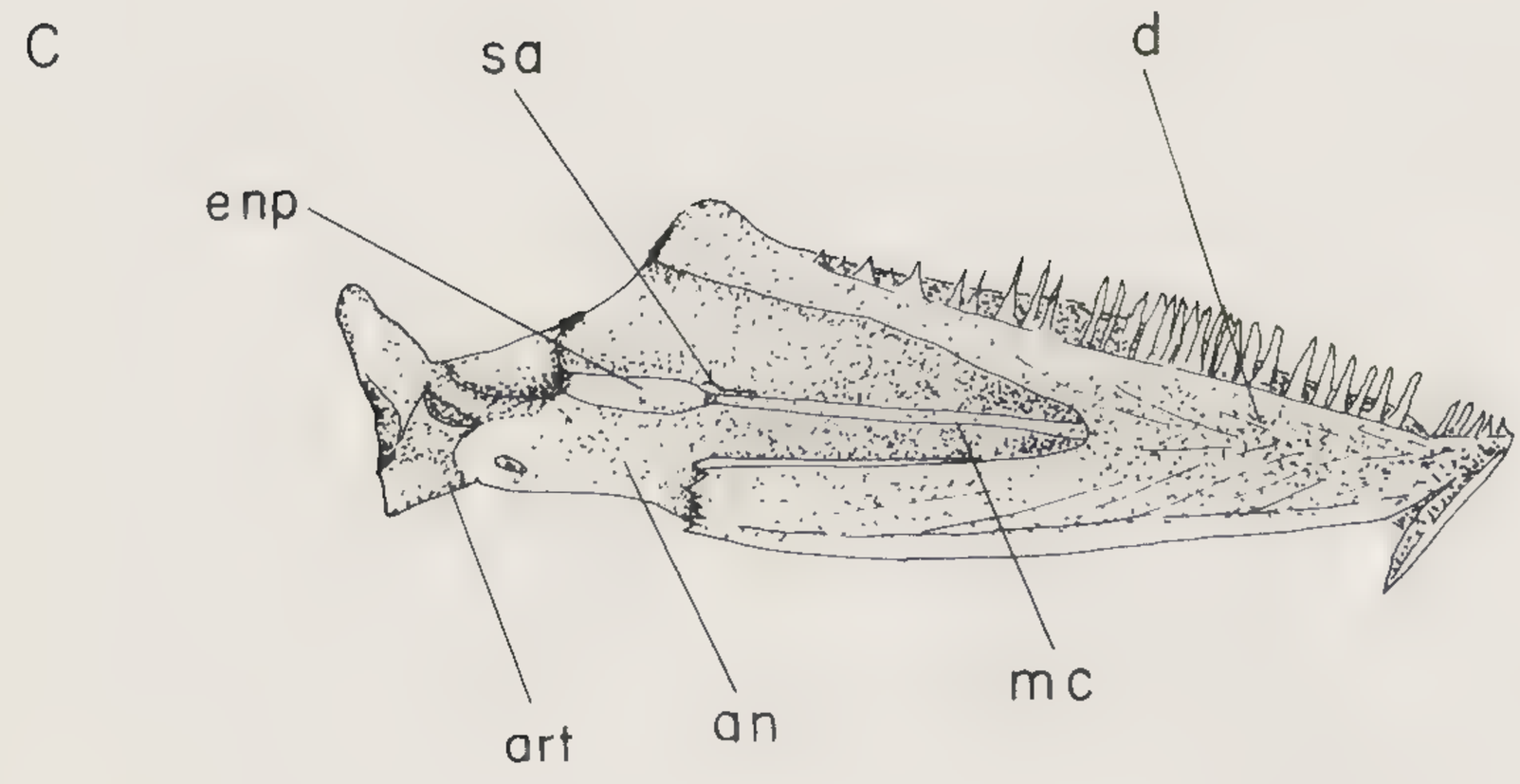

Fig. 6
Jaw elements from Specimen 1 with supporting detail from Specimens 8 to 14: *A*) left side; *B*) right side; *C*) medial view of left mandible.

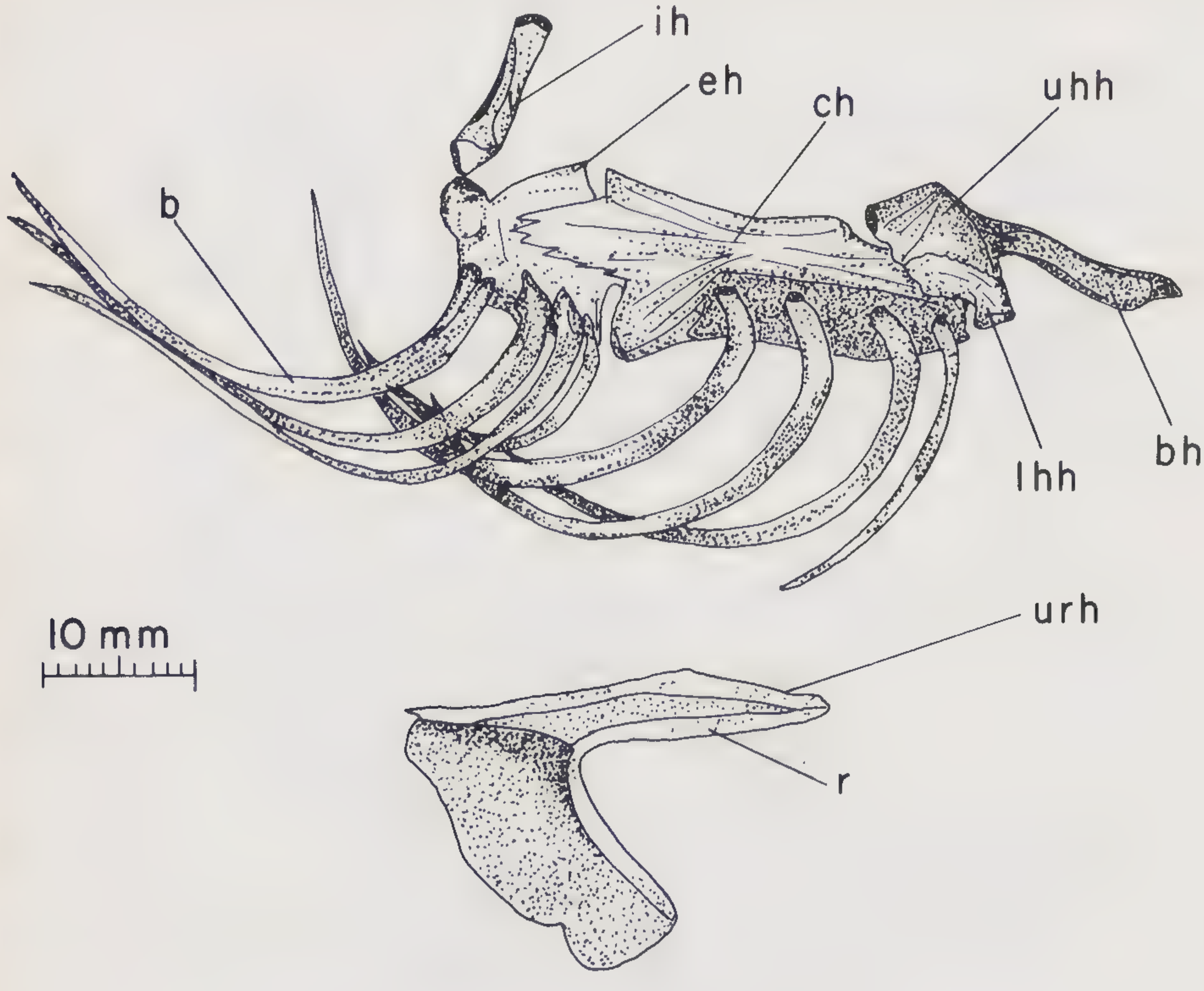

Fig. 7
Primary elements of the hyoid region excluding the hyomandibular from Specimen 1 and supporting detail from Specimens 6 and 7; right side.

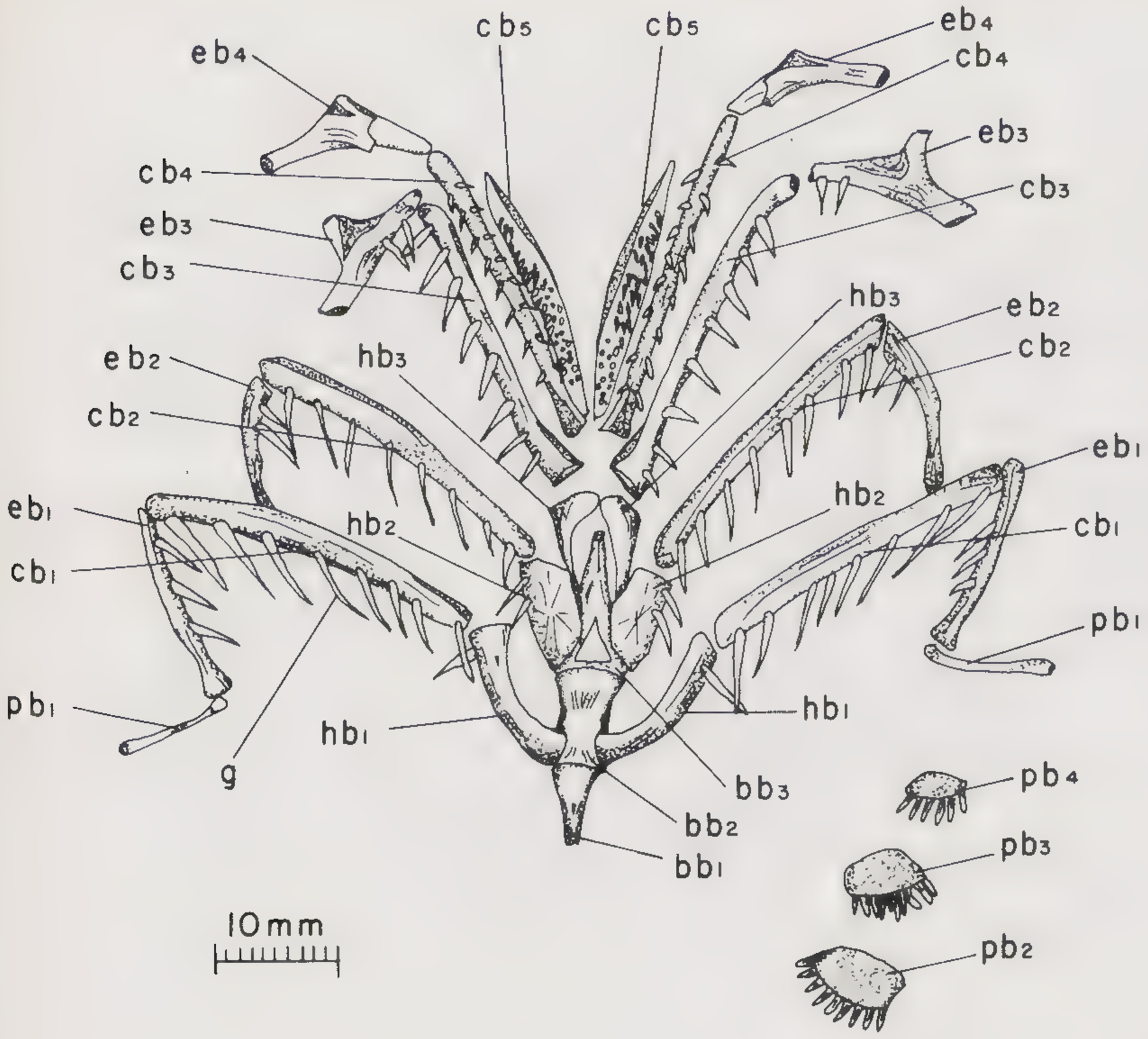

Fig. 8
Branchial region from Specimen 2.

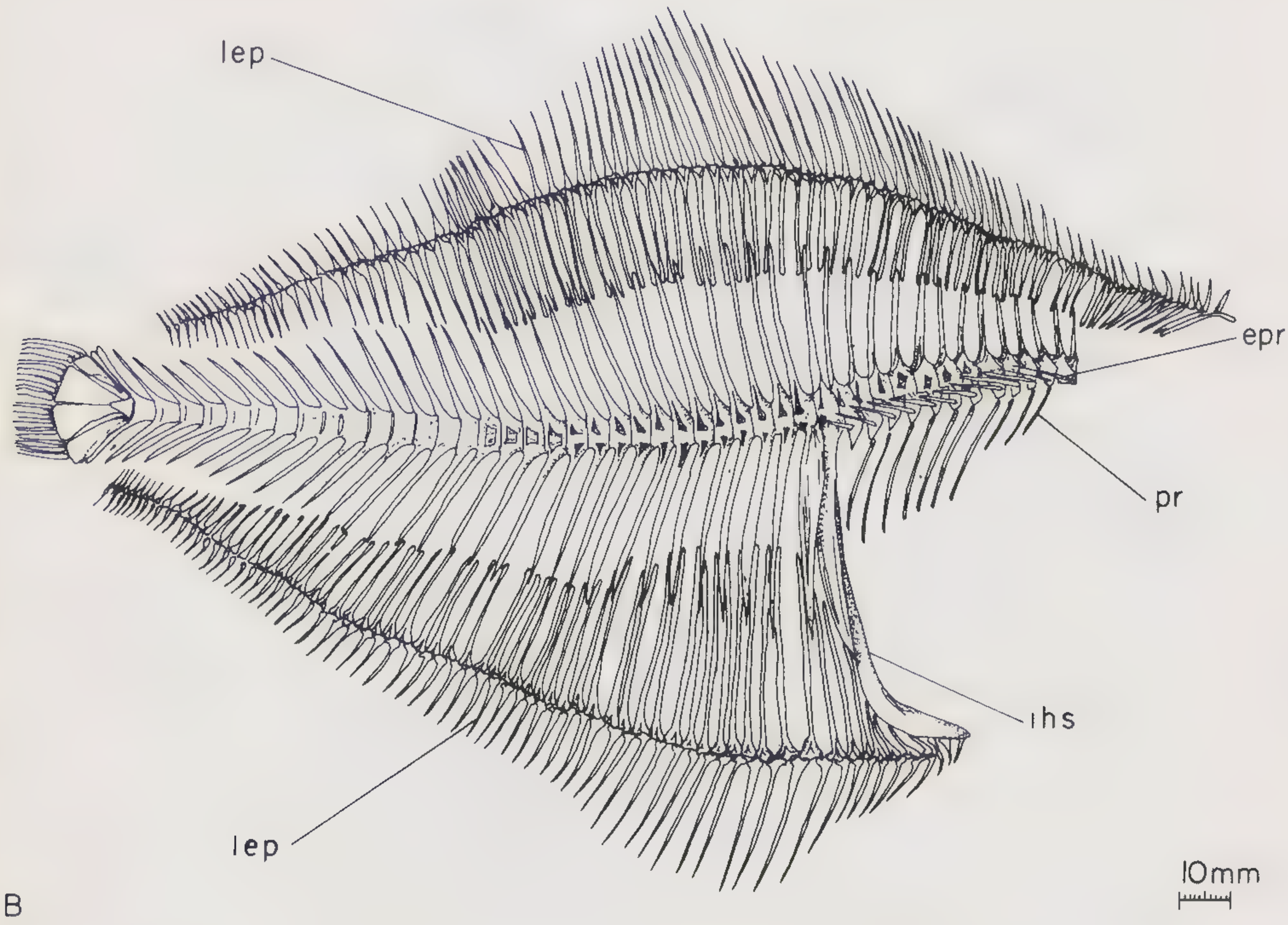

Fig. 9
The axial skeleton proportioned from several specimens. Trunk vertebrae right from first vertebra to vertebra with large interhaemal spine (*lhs*), which is the first caudal vertebra.

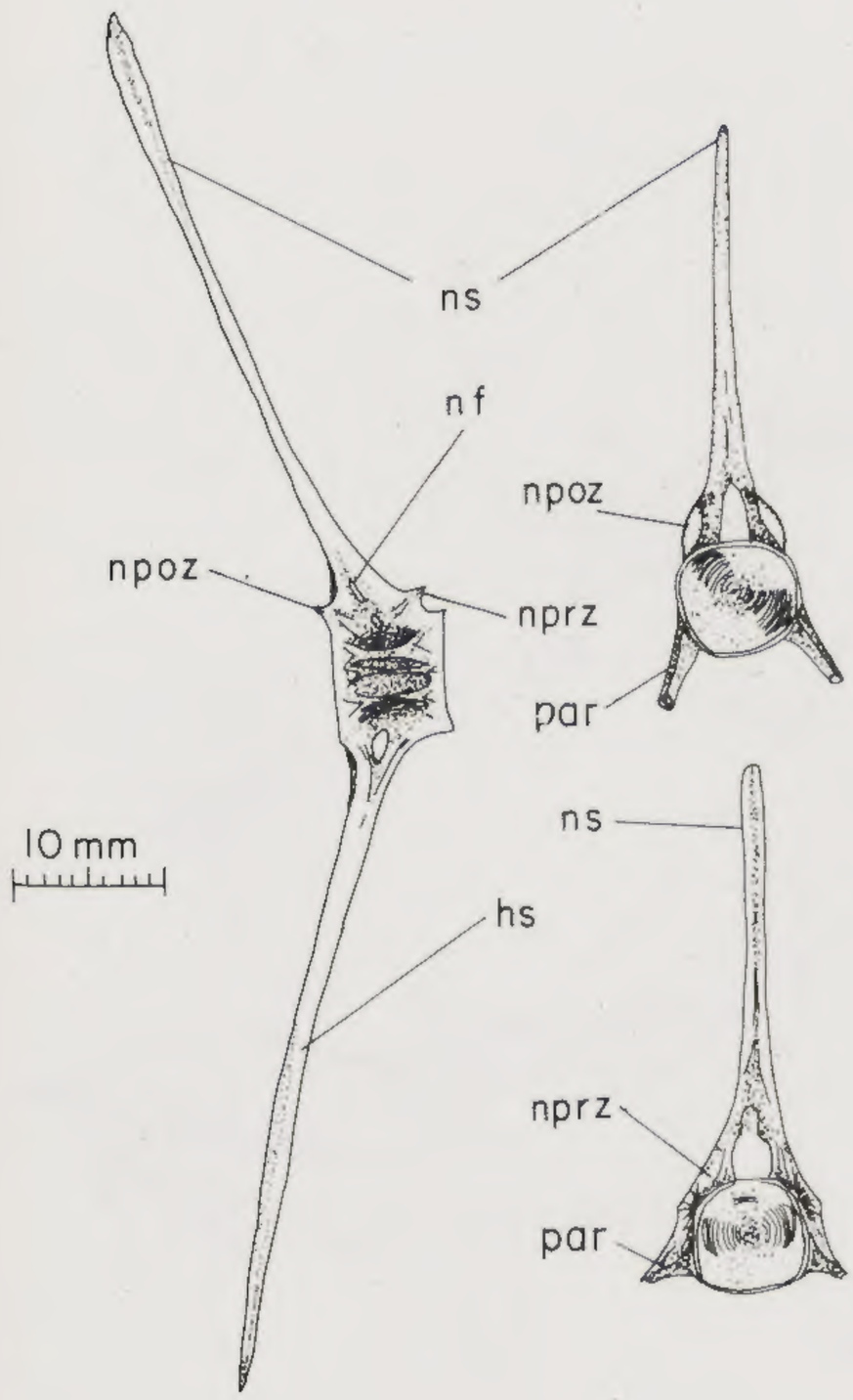

Fig. 10
Vertebrae and lepidotrichs from specimen, 851 mm total length: *A)* to the upper right: vertebra 4; to the right: vertebra 3 (trunk vertebrae); left, caudal vertebra 25. *B*) anal fin lepidotrichs 14, 15, 16, right to left.

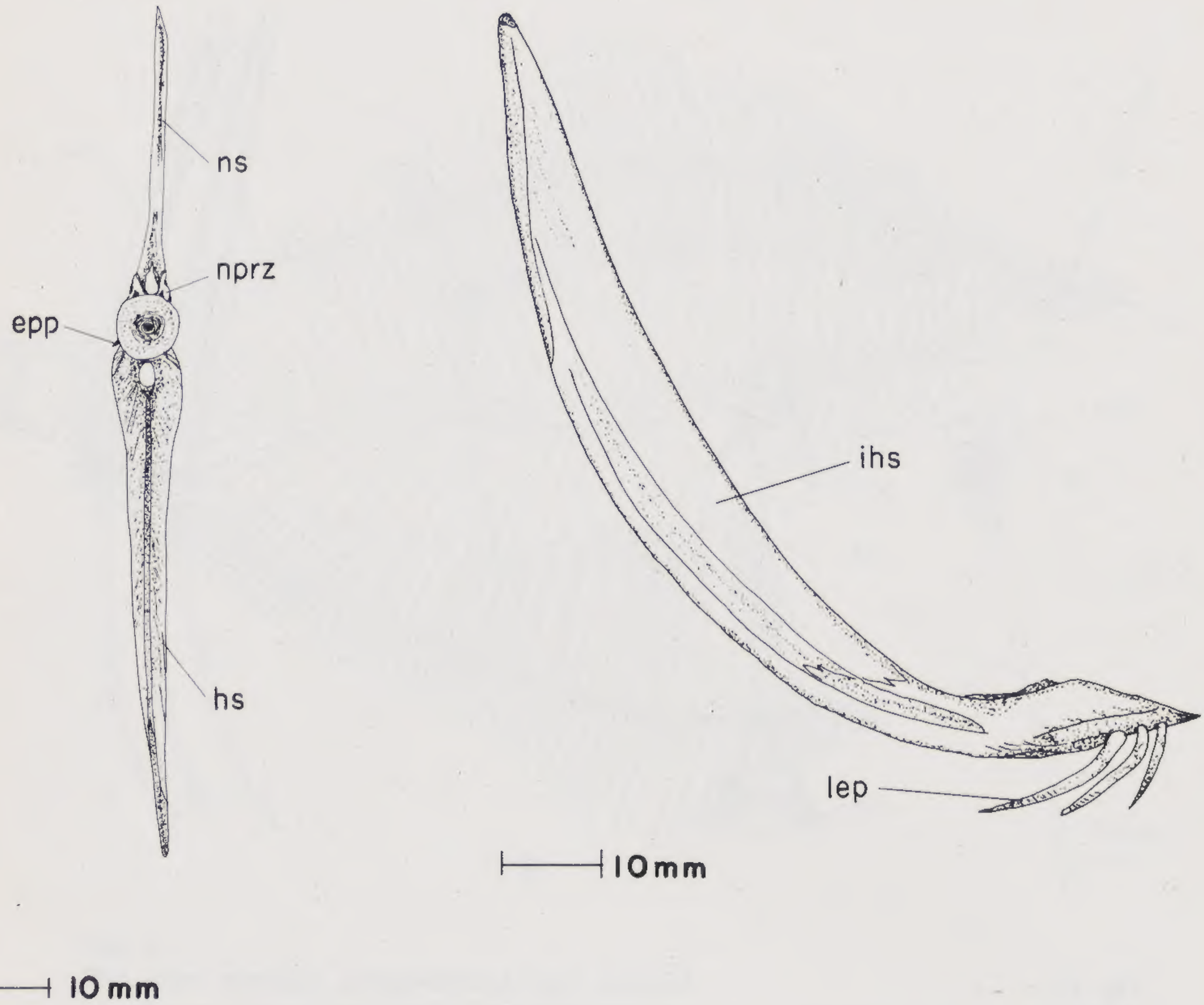

Fig. 11
Left, caudal vertebra 14; right interhaemal spine (ihs). Both figures proportioned from Specimen 1.

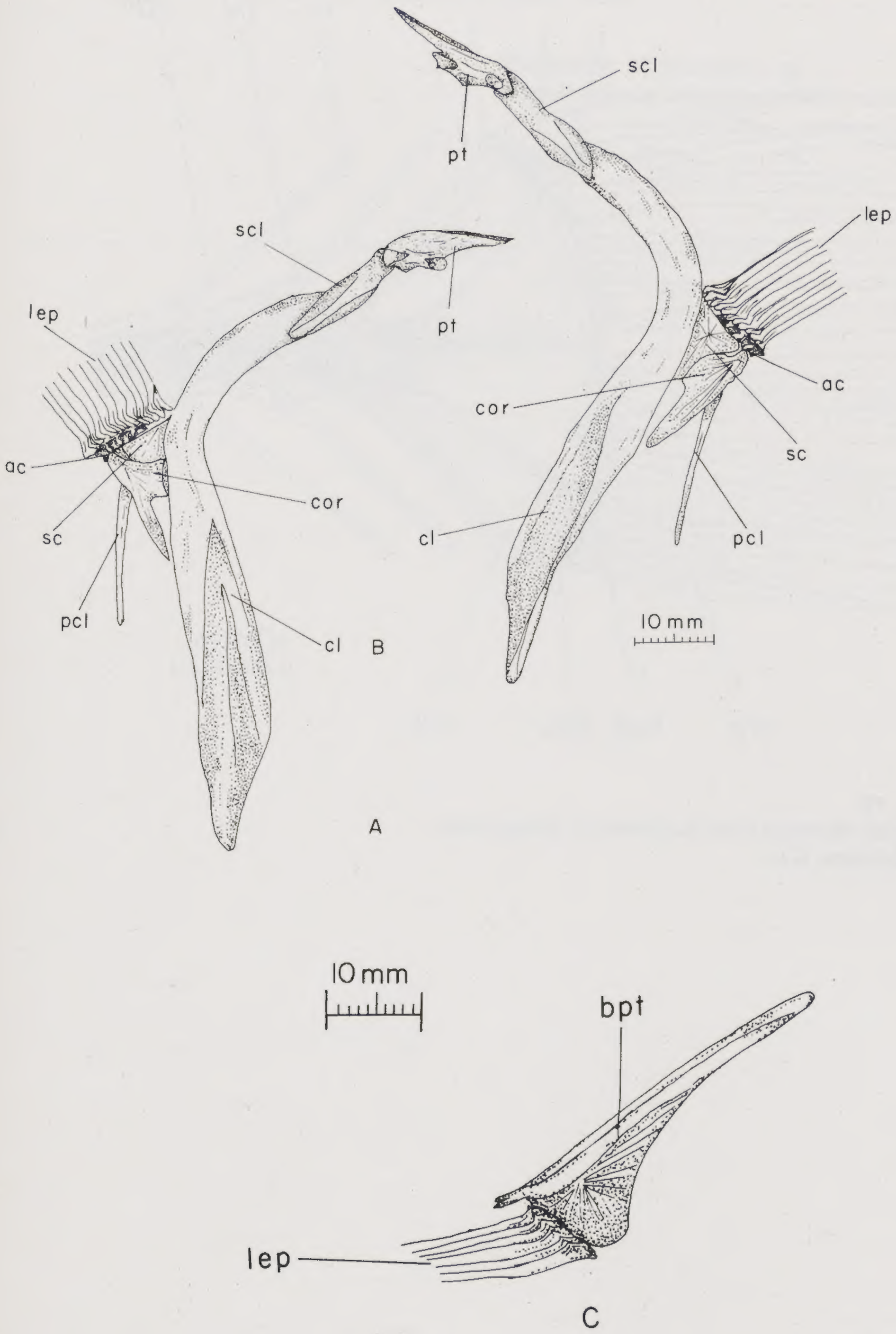

Fig. 12
Appendicular skeleton from Specimen 2. *A*) right side, pectoral girdle; *B*) left side, pectoral girdle; C) right side, pelvic girdle.

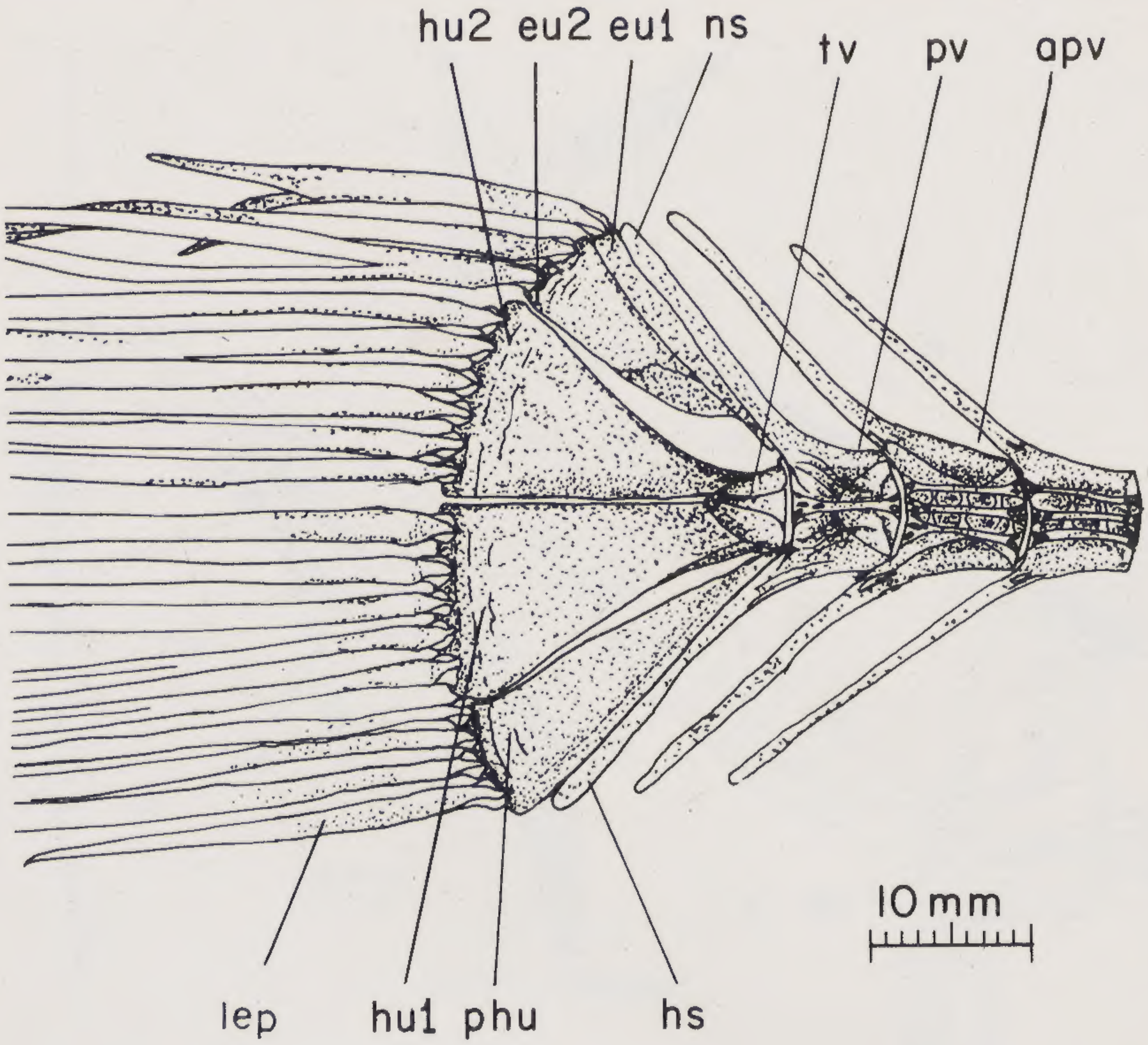

Fig. 13
Caudal skeleton from Specimen 2; details from specimens 6-14.